~~UNCLASSIFIED~~
~~CONFIDENTIAL~~

UNCLASSIFIED

RESEARCH MEMORANDUM

for the

Bureau of Aeronautics, Department of the Navy

INVESTIGATION OF THE KINGFISHER ~~CLASSIFYING TORPEDO~~ CLASSIFICATION CHANGED

IN THE LANGLEY FULL-SCALE TUNNEL - UNCLASSIFIED

TED NO. NACA BE-327

Langley Aeronautical Laboratory
Langley Air Force Base, Va.

FOR REFERENCE

NOT TO BE TAKEN FROM THIS ROOM

NATIONAL ADVISORY COMMITTEE
FOR AERONAUTICS

WASHINGTON

~~JUN 12 1948~~ OCT 6 1948

~~CONFIDENTIAL~~

~~UNCLASSIFIED~~

NATIONAL ADVISORY COMMITTEE FOR AERONAUTICS

Bureau of Aeronautics, Department of the Navy

INVESTIGATION OF THE KINGFISHER XAUM-2 FLYING TORPEDO IN THE LANGLEY FULL-SCALE TUNNEL - TED NO. NACA DE 327

By Bennie W. Cocke and U. Reed Barnett

SUMMARY

An investigation of a full-scale model of the Kingfisher XAUM-2 flying torpedo has been conducted in the Langley full-scale tunnel to determine the pressure recoveries available within the jet engine nacelle and to determine the effects of several changes in model configuration on the aerodynamic characteristics of the model. The effectiveness of elevons and tabs as control devices was also investigated.

The maximum pressure recovery measured at the compressor inlet in the engine nacelle was 0.51 percent of free-stream dynamic pressure for the cruise condition of the basic model. A fillet installed in the wing-fuselage juncture increased the available pressure recovery in the nacelle and reduced the drag of the model. The model had a high degree of static longitudinal stability for all configurations investigated. The elevons are effective lift producing devices and have little effect on the longitudinal trim of the model for the deflection range between -10° and 10°. Fixed tabs on the horizontal tail for longitudinal trim are ineffective for deflections between -3° and 3° but become fairly effective at higher deflections.

INTRODUCTION

At the request of the Bureau of Aeronautics, Department of the Navy, an investigation of a full-scale model of the Kingfisher XAUM-2 flying torpedo has been conducted in the Langley full-scale tunnel. A previous investigation was conducted on a $\frac{1}{2}$-scale XAUM-2 model at the David Taylor Model Basin (references 1 and 2), but because of model limitations, air-flow quantities through the engine nacelle during tests

were much too low to represent design operating conditions. The full-scale-tunnel investigation was therefore conducted to evaluate further the pressure recoveries available in the engine nacelle as well as to determine the aerodynamic characteristics of the model with nacelle air-flow quantities simulating design inlet-velocity ratios.

The investigation included the determination of (1) pressure recoveries within the jet engine nacelle for four inlet configurations, (2) the effects of several changes in model configuration on the aerodynamic characteristics of the model, and (3) the effectiveness of elevons and tabs as control devices.

COEFFICIENTS AND SYMBOLS

C_L	lift coefficient $\left(\frac{L}{qS}\right)$
C_D	drag coefficient $\left(\frac{D}{qS}\right)$
C_m	pitching-moment coefficient $\left(\frac{M}{qSc'}\right)$
C_l	rolling-moment coefficient $\left(\frac{L}{qSb}\right)$
C_n	yawing-moment coefficient $\left(\frac{N}{qSb}\right)$
C_h	hinge-moment coefficient $\left(\frac{H_a}{qb_a\bar{c}^2}\right)$
L	lift, pounds, or rolling moment, pound-feet
D	drag, pounds
M	pitching moment, pound-feet
N	yawing moment, pound-feet
H_a	aileron hinge moment, pound-feet
R	Reynolds number $\left(\frac{\rho V c'}{\mu}\right)$
q	dynamic pressure, pounds per square foot $\left(\frac{\rho V^2}{2}\right)$
p	static pressure, pounds per square foot

[redacted]

H	total pressure, pounds per square foot
ρ	mass density of air, slugs per cubic foot
μ	coefficient of viscosity, slugs per foot-second
V	air velocity, feet per second
S	wing area, square feet
c'	wing mean aerodynamic chord, feet
$\bar{c}$	root-mean-square chord of aileron aft of hinge line, feet
b	wing span, feet
α	geometric angle of attack referenced to torpedo center line, degrees
i_t	angle of incidence of horizontal tail referenced to torpedo center line, positive when trailing edge is down, degrees
δ_e	elevon deflection, positive when trailing edge is down, degrees
δ_t	tab deflection, positive when trailing edge is down, degrees

Subscripts:

o	free-stream conditions
i	nacelle inlet conditions
R	right-elevon conditions

APPARATUS

The Kingfisher XAUM-2 flying torpedo is a pilotless missile consisting of a standard Navy torpedo equipped with expendable wing, tail, and jet power-plant unit. The general arrangement and principal dimensions of the missile are shown in figure 1. The missile is designed to be air-launched and to operate at a constant airspeed of approximately 325 knots until its wings and power plant are detached at water entry for underwater approach to the target. Longitudinal and

lateral control in flight is furnished by means of full-span 20-percent-chord blunt trailing-edge elevons located along the wing trailing edge. Fixed tabs are incorporated in the horizontal tail to provide trim adjustments required by changes in model configuration.

The test model was furnished by the Bureau of Standards and consisted of a standard MK-13 Naval torpedo equipped with wing and tail. A nacelle for the jet power plant was attached to the the rear of the torpedo shroud ring and a detachable nose section to house control equipment was attached to the nose. As the jet power plant was not available, a blower was installed in the nacelle to provide a means of air-flow control and thus make possible a nacelle pressure-recovery investigation over a range of flow conditions. The general arrangement of the test nacelle is shown in figure 2. For the investigation, the underwater propellers (fig. 2) were locked with the blades alined with the torpedo fins.

The Kingfisher model was mounted for tests on a single-strut support system in order to minimize the tare and interference effects. The single-strut support was also selected to provide for an auxiliary strain-gage balance system mounted within the model and on the flight center of gravity for determining the aerodynamic moments of the model. A general view of the model as mounted for testing is presented in figure 3.

TESTS

The initial phase of the investigation was the evaluation of three nacelle inlet configurations furnished with the model. These inlets designated as the MK-13, the MK-21, and the shroud ring cowl are shown in figure 4. A fourth configuration designated as the modified shroud ring was also tested and is shown in figure 4. In order to evaluate each inlet configuration, total- and static-pressure measurements were obtained at the compressor inlet station (fig. 2) with the model set at tunnel angles of attack of -4°, 0°, and 4° for each configuration. At each angle of attack the air-flow quantity was varied to determine the effect of inlet-velocity ratio. For each condition investigated, total pressure was also measured at the nacelle inlet station (fig. 2), but because of unstable flow at the inlet, accurate evaluation of these pressures was not possible. In addition to these basic tests, pressure measurements were also made to determine the effects on pressure recovery of a wing fillet (fig. 5), a modified nose fairing (fig. 6), and of sealing and fairing the gaps in the torpedo body.

The second phase of the investigation consisted of force tests over the angle-of-attack range from 4° to -4° to determine longitudinal

aerodynamic characteristics. During all force tests the air flow through the nacelle was maintained at flow quantities corresponding to the design inlet-velocity ratios. The tests were arranged to determine the effects on lift, drag, and pitching moment of four nacelle inlet configurations (fig. 4), a wing fillet (fig. 5), a modified nose section (fig. 6), a tail fillet (fig. 7), under-wing control actuators (fig. 8), under-wing altimeter antennas (fig. 8), an auxiliary generator (fig. 9), and an alternate horizontal-tail position (fig. 9).

The third phase of the investigation consisted of tests to determine the effectiveness of elevons and tabs for producing longitudinal trim. The force, moment, and hinge-moment characteristics of the model with the full-span elevon deflected were determined for angles of attack of 0°, ±2°, and ±4°. At each angle of attack, measurements were made for a range of elevon deflections from -40° to 40°. The tab-effectiveness tests were made over the same range of angles of attack and for a tab-deflection range from -15° to 15°. In addition to these longitudinal-control-effectiveness tests, one additional test was made with the left elevon fixed at zero deflection while the right elevon was deflected through a range between -30° and 30° to determine its effectiveness as a lateral-control device. All tests were made at a tunnel airspeed of approximately 56 miles per hour which corresponds to a Reynolds number of approximately 1,400,000 based on a mean aerodynamic chord of 2.66 feet. Aerodynamic moments are presented about the normal-flight center of gravity located on the torpedo center line and 79.25 inches forward of the aft end of the torpedo.

RESULTS AND DISCUSSION

All test results have been corrected for jet-boundary, blocking, stream-angle, and tare effects. Drag results have also been corrected for the thrust tares resulting from effects of the blower operation.

Nacelle Investigation

The most important results of the pressure investigation within the engine nacelle at the compressor station (fig. 2) are summarized in figures 10 to 13. Figure 10 shows the effect of variation of inlet-velocity ratio on pressure recovery for the MK-13, MK-21, and modified-shroud-ring inlets. These results indicate that, for the design flight attitude, maximum possible recoveries are 51 and 50 percent for the MK-13 and MK-21 inlets, respectively, and show that design velocity ratios for each of these inlets (0.36 for the MK-13 and 0.45 for the MK-21) are slightly below optimum for maximum recovery. The Bureau of Standards shroud cowl (results not shown) had very low and nonuniform

[redacted]

recoveries because of its high design inlet-velocity ratio (0.9), inefficient internal diffusion, and complete immersion of the narrow annular inlet in the very low energy region of the torpedo boundary layer. The modified shroud inlet was obtained by increasing the inlet diameter of the shroud cowl to provide a lower design inlet-velocity ratio (0.7), and, at the same time, to allow the inlet to take in a portion of its air from a higher energy region of the boundary layer. With the best diffuser available, within the space limitations, recoveries of 47 percent were obtained with this inlet. The low recoveries (51 percent maximum) for these nacelle inlets are primarily the results of the thick boundary-layer conditions at the inlet in its present location. It would be possible to obtain some increase in pressure recovery if it were mechanically feasible to use suitable boundary-layer removal scoops on the torpedo body; however, surveys indicate that the boundary layer over the aft section of the torpedo is so thick (up to 6 in. at the test Reynolds number) that optimum inlet recoveries could not be obtained for any configuration similar to the present basic design.

The distribution of total-pressure coefficient $\left(\frac{H - P_o}{q_o}\right)$ at the compressor inlet station for the MK-13 and MK-21 inlet configurations is shown in figures 11 and 12, respectively. Data are presented for each inlet with and without a fillet installed in the wing-fuselage juncture. These results show that for cruise attitude of the missile (α about -0.6°) there will be some asymmetry of pressure distribution at the compressor. Tuft surveys made in conjunction with these tests indicated that torpedo boundary-layer conditions just ahead of the inlet are so critical that separation occurs on the lower torpedo surface at small negative angles of attack of the missile. The upper surface is not so critical because of the stabilizing effects of downwash from the wing.

The variation of total-pressure recovery with angle of attack with and without the under-wing fillet (fig. 13) shows that the addition of a fillet in the wing-fuselage juncture increases the maximum available recoveries for each inlet configuration and also eliminates most of the adverse effects of increasing angle of attack. The installation of a modified nose accessory section and the sealing and fairing of the torpedo body had very little effect on the nacelle pressure recoveries.

The results of the nacelle investigation indicate that the maximum pressure recovery available at $\alpha = -0.6^\circ$ is $0.58q_o$ and is obtained for the MK-21 inlet with a fillet installed in the wing-fuselage juncture. With the present model configuration, it will not be possible to obtain much greater recoveries because of extremely thick boundary-layer conditions over the rear of the torpedo body and because of the interference effects from the wing located just ahead of

the inlet. Of the various modifications investigated, only the wing fillet produced any appreciable gain in pressure recovery.

Drag

The results of drag measurements obtained for the several model configurations are summarized in table I. Corrections for the effects of blower operation have been applied to all drag results using the equation $\Delta D = M\left(\sqrt{\frac{H_e - P_o}{1/2\ \rho}} - \sqrt{\frac{H_c - P_o}{1/2\ \rho}}\right)$ where M is the mass of air handled, H_e is the total pressure in the nacelle exit, and H_c is the total pressure at the compressor inlet station (fig. 2). The drag coefficients presented therefore include the external drag of the model plus the internal drag from the nacelle inlet to the compressor inlet station. The drag results indicate that, for a lift coefficient of 0.25 corresponding to design operating conditions of the missile, the basic model has a drag coefficient of 0.060 with either the MK-13 or MK-21 inlets installed. This drag coefficient was reduced to 0.056 by the addition of the fillet in the wing-fuselage juncture but no further reduction was shown for the addition of a tail fillet. As shown in the table, installing such accessories as under-wing actuators, altimeter antennas, and wind generator resulted in adding a total drag increment of 0.009. No appreciable change in drag was found with the modified nose installed nor with the MK-21 tail configuration.

Longitudinal Aerodynamic Characteristics

The variations of pitching-moment, lift, and drag coefficients with angle of attack for each of the model configurations investigated are shown in figures 14 to 21. Table II summarizes the effects on lift and pitching-moment coefficients for each configuration change. Values of pitching-moment and lift coefficients shown in the table are for a model angle of attack of -0.8° which corresponds to the design flight lift coefficient ($C_L = 0.25$) of the basic model. Also shown in the table are values of $dC_m/d\alpha$ and the change in pitching-moment coefficient for each configuration investigated.

The model has a large amount of static longitudinal stability for all configurations investigated $\left(\text{minimum value } \frac{dC_m}{d\alpha} = -0.068\right)$. The results indicate that the basic model with the present stabilizer setting $i_t = 0^\circ$, is out of trim by a ΔC_m of 0.082 at the design lift coefficient of 0.25 (fig. 14). It should be pointed out that the stabilizer on the test model was twisted approximately $\frac{1}{2}^\circ$ and the absolute values of pitching-moment coefficient may not apply exactly to

[redacted]

succeeding flight models. The increments of pitching-moment coefficient shown for changes in model configuration, however, should not be affected by this degree of stabilizer twist.

The longitudinal stability of the model was not appreciably affected by any of the modifications tested, although several changes in trim are indicated. The addition of the wing fillet and the tail fillet each caused a change in trim of $-0.0017C_m$. (See figs. 15 and 16.) The under-wing actuators did not affect model trim, but an increment in C_m of -0.027 resulted from the addition of the altimeter antennas. (See figs. 17 and 18.) Trim changes are also indicated for the wind generator and for the MK-21 tail configuration in figures 19 and 21.

Elevon Effects

The results of tests made to determine the effect of elevon deflection on the aerodynamic characteristics of the model (fig. 22) show that the elevons are quite effective as lift producing devices throughout their deflection range. It is also noted that for the deflection range from -10° to 10° very little change in pitching moment occurs. At the higher positive and negative deflections, larger changes in trim are shown, but the maximum average value of $dC_m/d\delta_e$ never exceeds 0.0045. Within the range investigated, angle of attack had little effect on the lift effectiveness of the elevons.

Of possible interest from trim considerations is the reversed elevon effectiveness in which positive or downward elevon deflections produce more positive pitching moments and, conversely, up elevon deflection results in negative moments. Although there are no conclusive measurements to indicate the cause for this reversal in effectiveness, it is considered that, from the geometry of the model and from observations of the influence of the wing downwash on the flow about the rear of the torpedo, small downwash changes at the tail would produce pitching moments that predominate over the small wing pitching moments produced by deflection of the short-coupled elevon flaps. The effectiveness of the small fixed tabs on the tail in producing trim changes, as shown in the next section, gives evidence of the sensitivity of the horizontal tail to small changes in relative angle of attack in producing pitching moment.

Tab Effectiveness

The results of the trim-tab-effectiveness tests showing variations of C_L, C_D, and C_m with tab deflection for the MK-13 and MK-21 torpedo configurations are presented in figures 23 and 24, respectively. The tabs are relatively ineffective for the deflection range from -3° to 3°,

but, for the higher deflections, the tabs become more effective with values of $dC_m/d\delta_t$ of approximately -0.015 for down deflections greater than 7° and -0.010 for up deflections.

Angle-of-attack variation had little effect on tab effectiveness within the range of tab deflections investigated. It is also noted that the effectiveness was approximately equal for both the MK-13 and MK-21 torpedo configurations.

Aileron Effectiveness

The full-span elevons are effective as ailerons as shown by the stable linear curve of C_l against δ_{e_R} in figure 25. For maximum total deflection of 60°, the increment of rolling-moment coefficient is 0.069, which should be adequate for control of lateral motions of the missile. The yawing-moment coefficient due to aileron deflection is favorable over most of the deflection range but of small magnitude and would have little significance in view of the high degree of directional stability shown in the $\frac{1}{2}$-scale model tests of references 1 and 2.

The elevon hinge-moment characteristics (fig. 26) show an approximately linear variation although the rate of change of C_h with δ_e between $\pm 10^\circ$ is approximately half that at the higher deflections. For the most part, there is little variation of C_h with α throughout the angle-of-attack range investigated.

SUMMARY OF RESULTS

1. For the nacelle configurations investigated, the maximum pressure recovery obtained at the compressor inlet in the engine nacelle was $0.51q_o$ at cruise attitude.

2. Installing a fillet in the wing-fuselage juncture increases the available nacelle pressure recovery and reduces the drag of the model.

3. The model has a large degree of static longitudinal stability for all configurations investigated.

[redacted]

4. The elevons are effective lift producing devices and for the deflection range from -10° to 10° have little effect on longitudinal trim.

5. The tabs on the horizontal tail are ineffective at low deflections (±3°) but at high deflections produce values of $dC_m/d\delta_t$ as high as -0.015 for down deflections and 0.010 for up deflections.

6. The elevon is effective as an aileron and has essentially linear rolling-moment and hinge-moment variations with control deflection.

Langley Aeronautical Laboratory
National Advisory Committee for Aeronautics
Langley Air Force Base, Va.

Bennie W. Cocke
Aeronautical Research Scientist

U. Reed Barnett
Aeronautical Research Scientist

Approved: Clinton H. Dearborn
Clinton H. Dearborn
Chief of Full-Scale Research Division

GMF

REFERENCES

1. Blalock, James E., and Payne, W. Randolph: Wind-Tunnel Tests of a 1/2-Scale Model of the XAUM-2 Kingfisher C Pilotless Aircraft. Part I - Preliminary Longitudinal Tests - TED No. TMB DE 318. Rep. C-70 Aero 750, David Taylor Model Basin, Navy Dept., Jan. 1948.

2. Blalock, James E., and Payne, W. Randolph: Wind-Tunnel Tests of a 1/2-Scale Model of the XAUM-2 Kingfisher C Pilotless Aircraft. Part II - Stability and Control Tests - TED No. TMB DE 318. Rep. C-71 Aero 750, David Taylor Model Basin, Navy Dept., Jan. 1948.

[redacted]

TABLE I.- SUMMARY OF DRAG MEASUREMENTS

Test	Configuration	C_L	C_D
1	MK-13 basic configuration	0.25	0.060
2	Same as 1 except MK-21 inlet installed	.25	.060
3	Same as 1 except wing fillet installed	.25	.056
4	Same as 3 except tail fillet installed	.25	.056
5	Same as 4 except under-wing actuators installed . .	.25	.057
6	Same as 5 except altimeter antennas installed . . .	.25	.059
7	Same as 6 except wind generator installed	.25	.065
8	Same as 7 except modified nose installed	.25	.065
9	Same as 7 except MK-21 torpedo configuration . . .	.25	.064

NACA

TABLE II.- SUMMARY OF TRIM CHANGES FOR SEVERAL MODEL CONFIGURATIONS

Run	Condition	C_L at $\alpha = -0.8^\circ$	C_m	ΔC_m	$dC_m/d\alpha$
1	Basic MK-13 configuration	0.25	0.082	-----	-0.068
2	Same as 1 except wing fillet installed	.23	.065	-.017	-.069
3	Same as 2 with tail fillet	.24	.038	-.017	-.068
4	Same as 3 except under-wing actuators installed	.25	.037	0	-.072
5	Same as 4 except altimeter antennas installed	.25	.010	-.027	-.072
6	Same as 5 with wind generator added .	.25	0	-.010	-.074
7	Same as 6 with modified nose installed	.26	0	0	-.075
8	Same as 7 except MK-21 tail configuration	.23	.017	.017	-.075

NACA

[redacted]

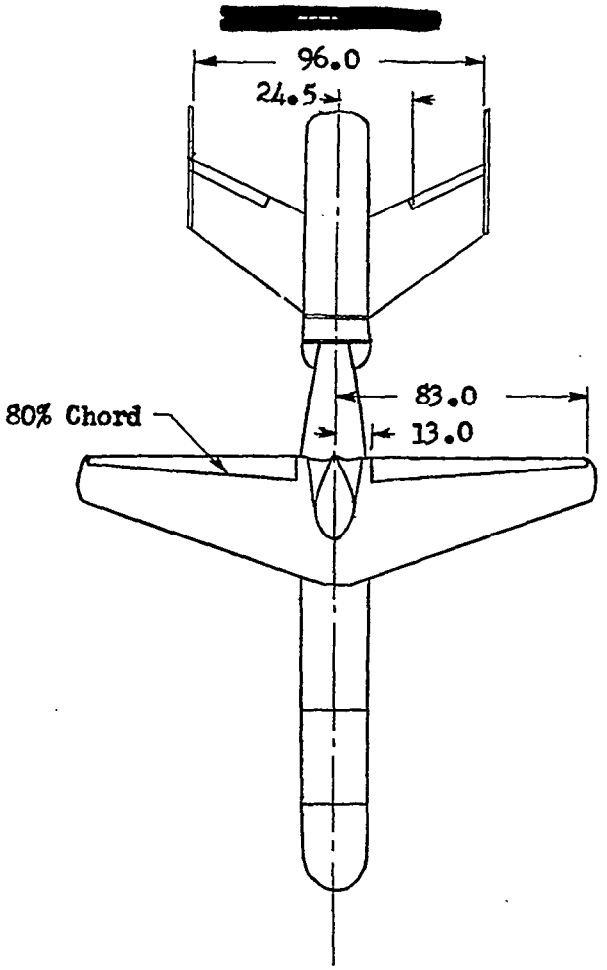

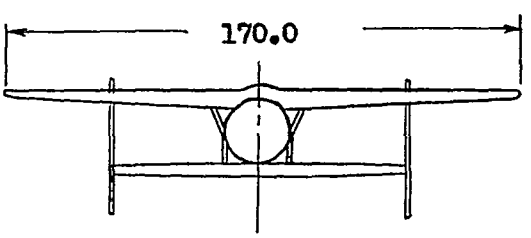

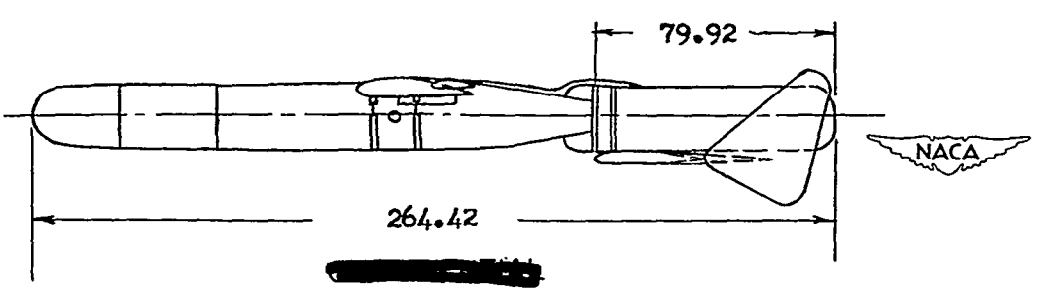

Wing

Area, sq ft	34.68
Root chord, ft	3.86
Tip chord, ft	1.20
MAC, ft	2.66
Airfoil Section	N.B.S. 700

Elevon

Area aft of hinge line, sq ft	2.80
Root-mean-square chord, ft	0.47

Horizontal Tail

Area, sq ft	20.00
Root chord, ft	3.00
Tip chord, ft	2.00
Tab area, sq ft (1)	0.56
Airfoil Section	NACA 0012

Vertical Tail

Area, sq ft	14.00

All dimensions in inches

Figure 1.– Principal dimensions of the Kingfisher XAUM–2, model C.

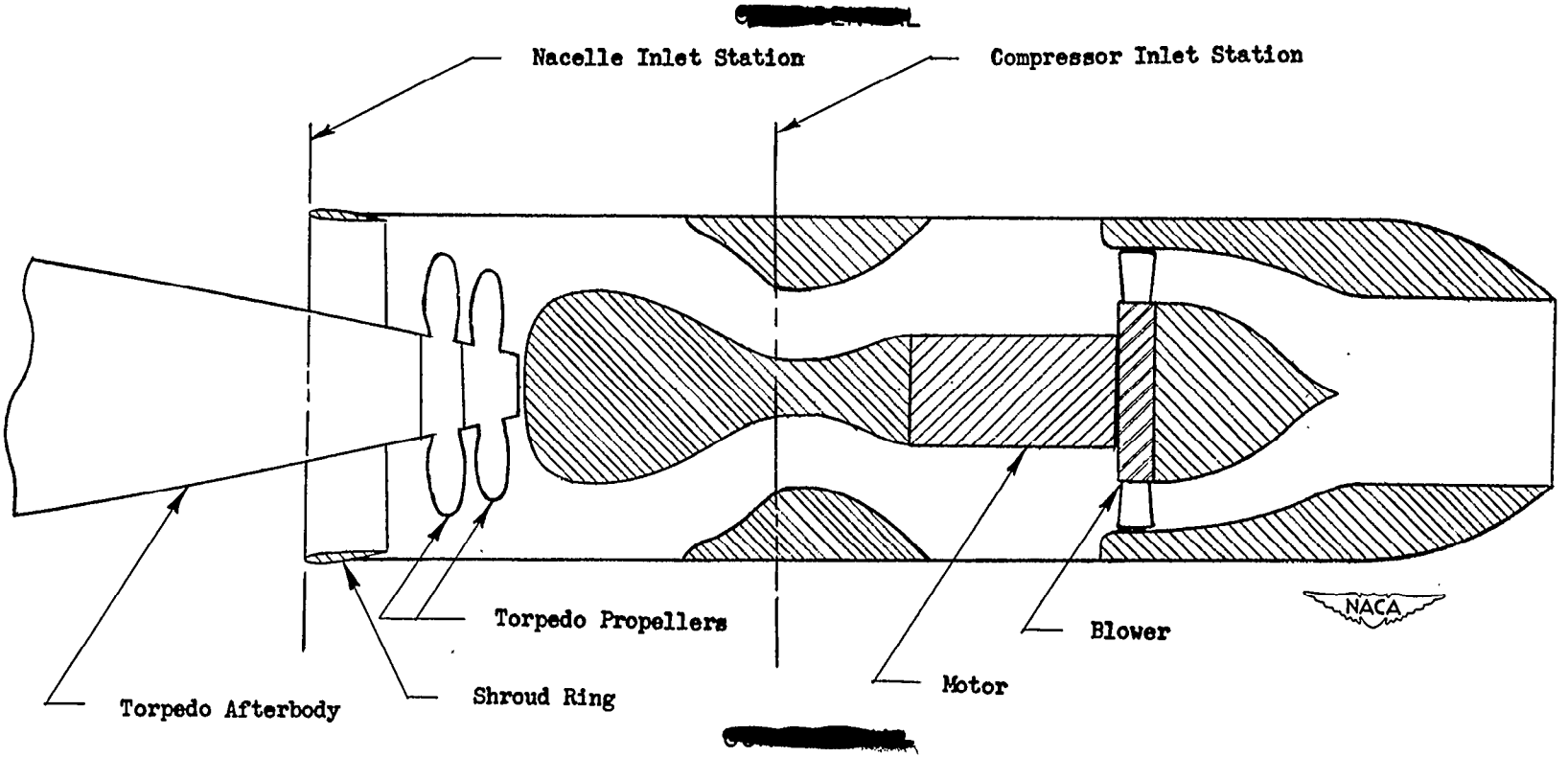

Figure 2.— Layout of Kingfisher nacelle as tested in Langley full-scale tunnel.

[redacted]

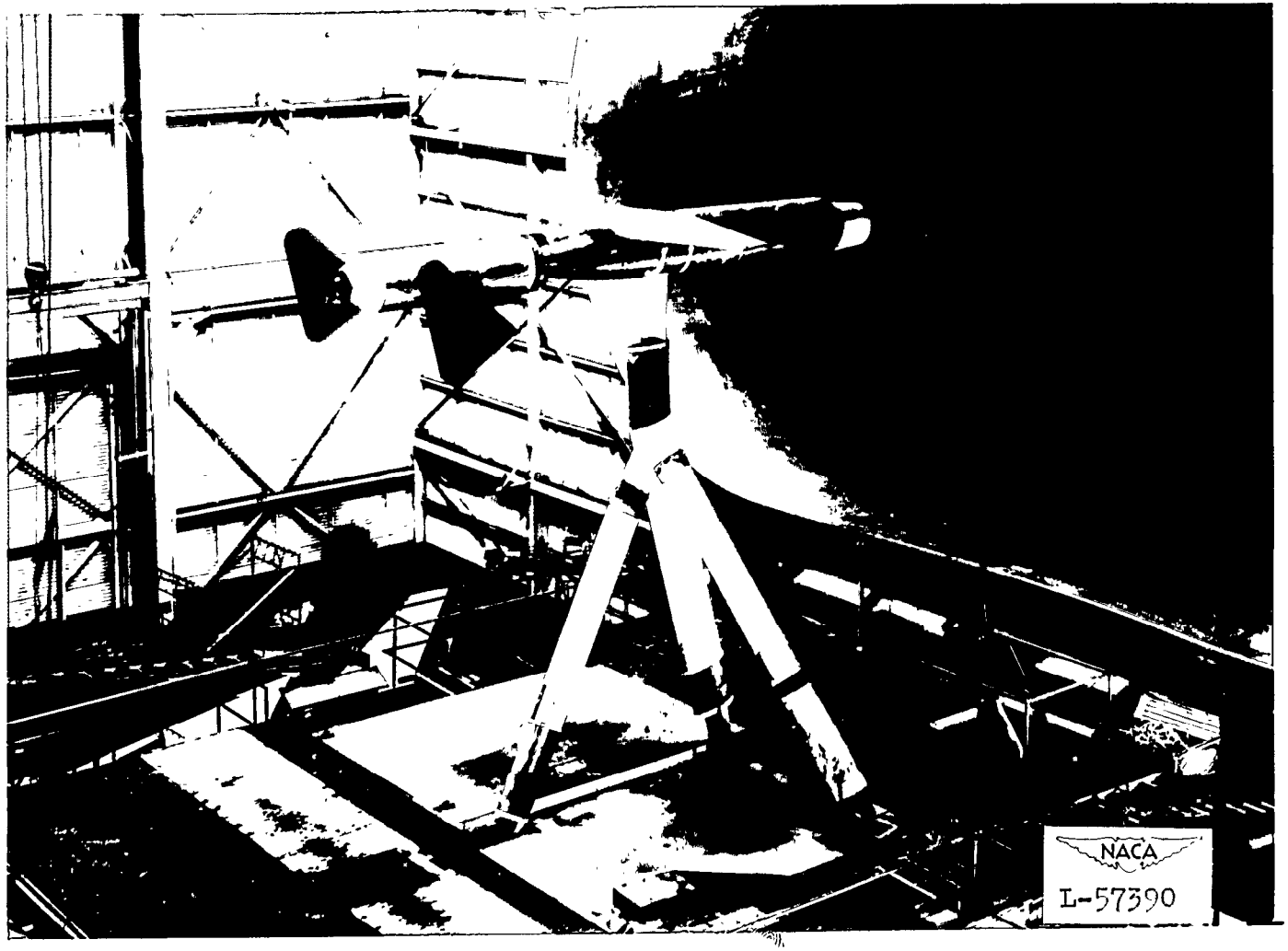

Figure 3.- Kingfisher XAUM-2 mounted for test in the Langley full-scale tunnel.

[redacted]

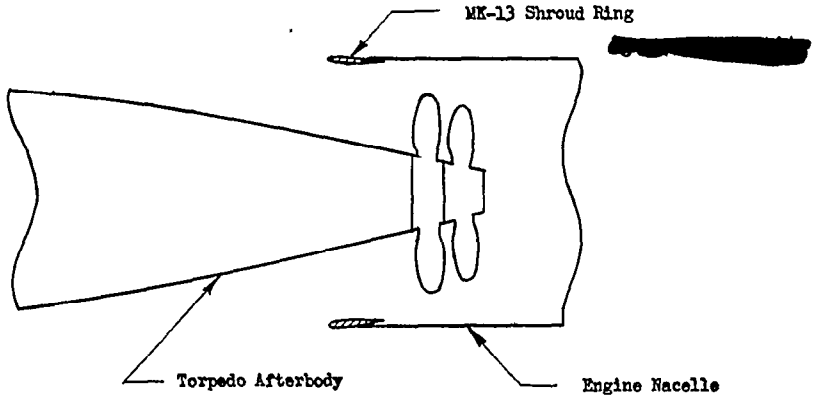

MK-13 Torpedo Configuration

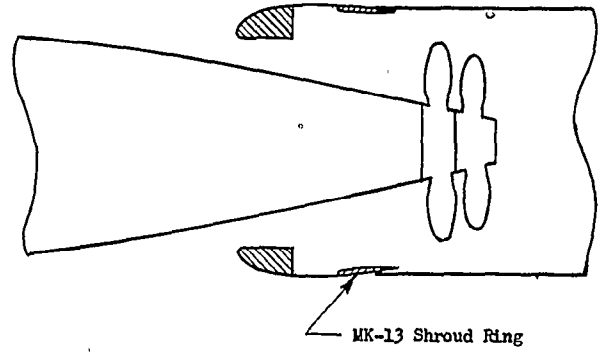

Shroud Ring Cowl Configuration

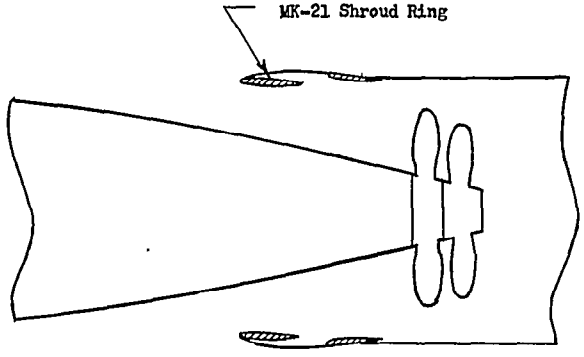

MK-21 Torpedo Configuration

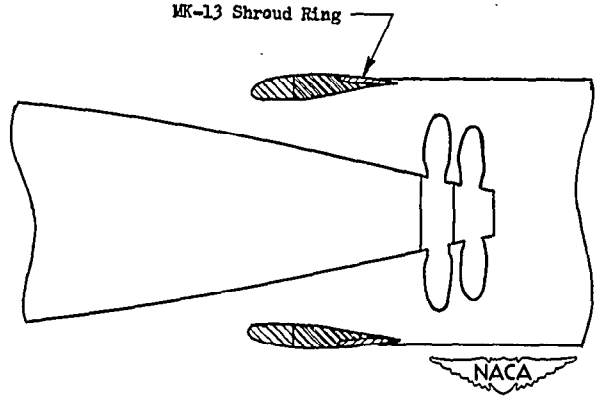

Modified Shroud Ring Cowl Configuration

Figure 4.— Air-inlet configurations investigated on Kingfisher XAUM-2, model C.

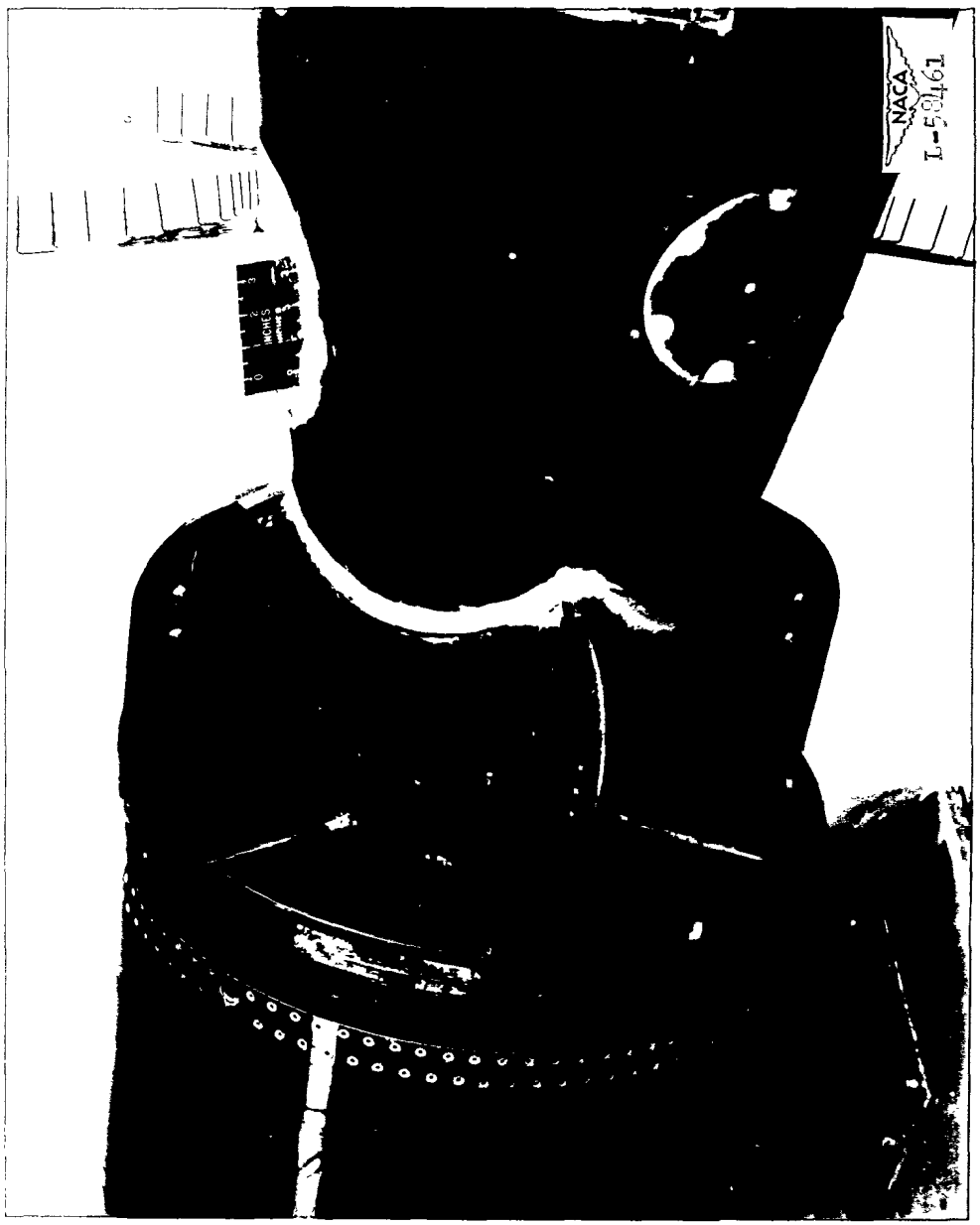

MK-13 Inlet

Figure 4.- Continued.

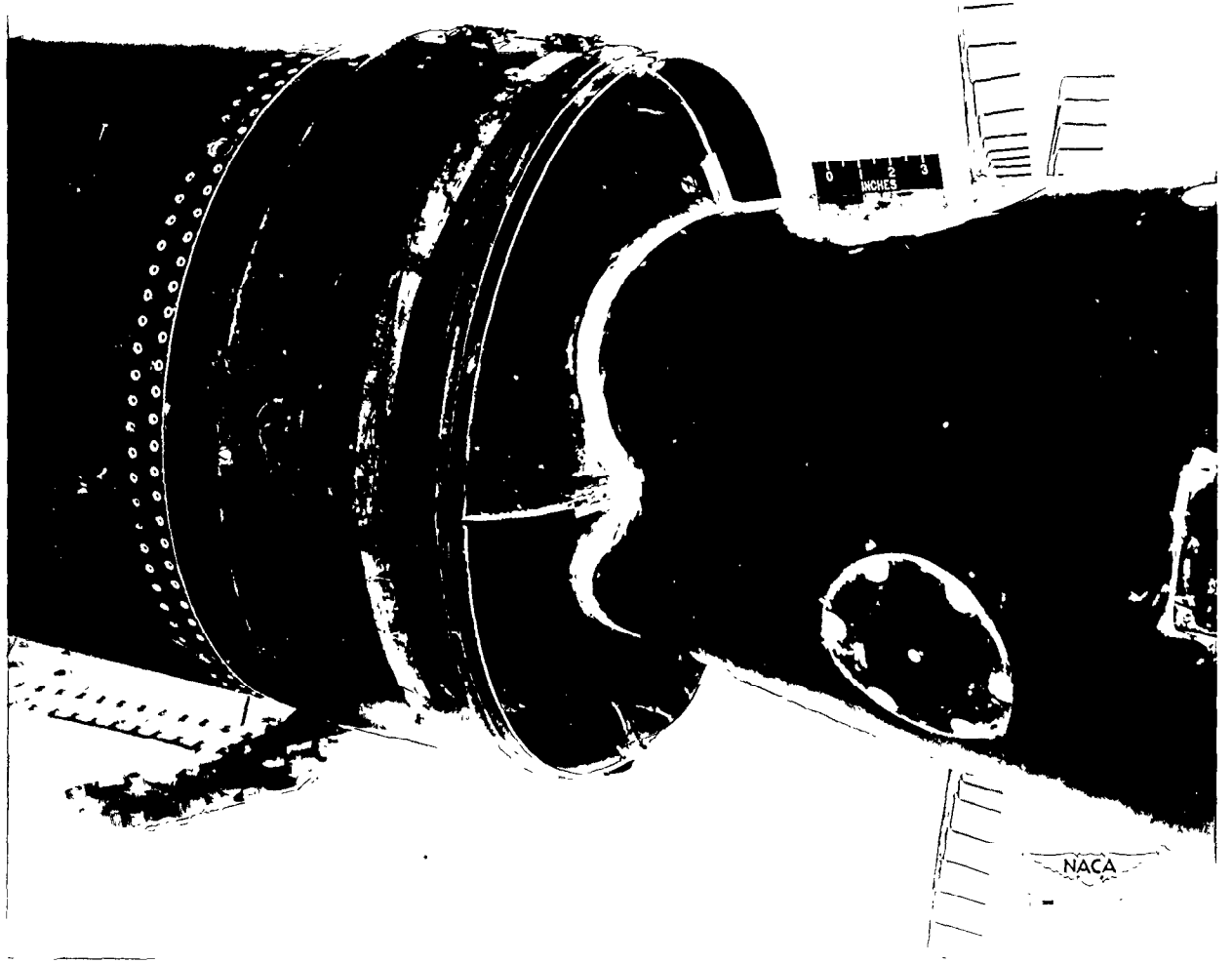

MK-21 Inlet

Figure 4.- Continued.

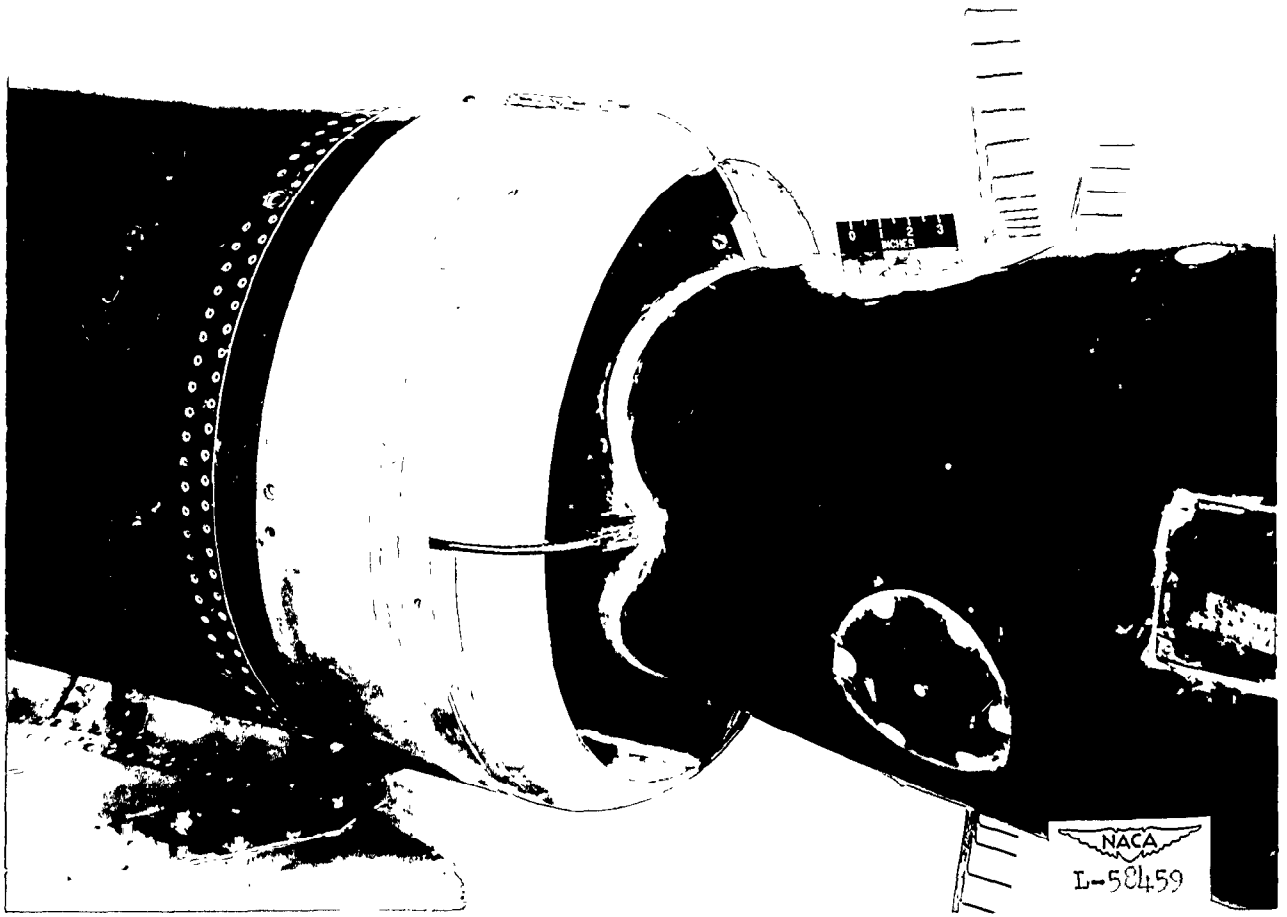

Modified Shroud Cowl

Figure 4.– Concluded.

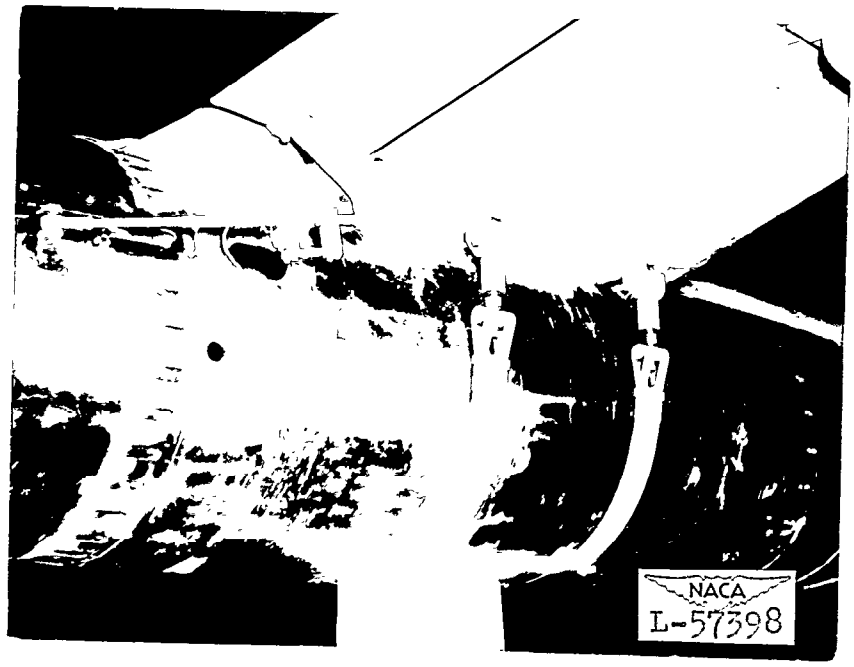

(a) Basic condition.

(b) Fillet installed.

Figure 5.— Wing–fuselage juncture.

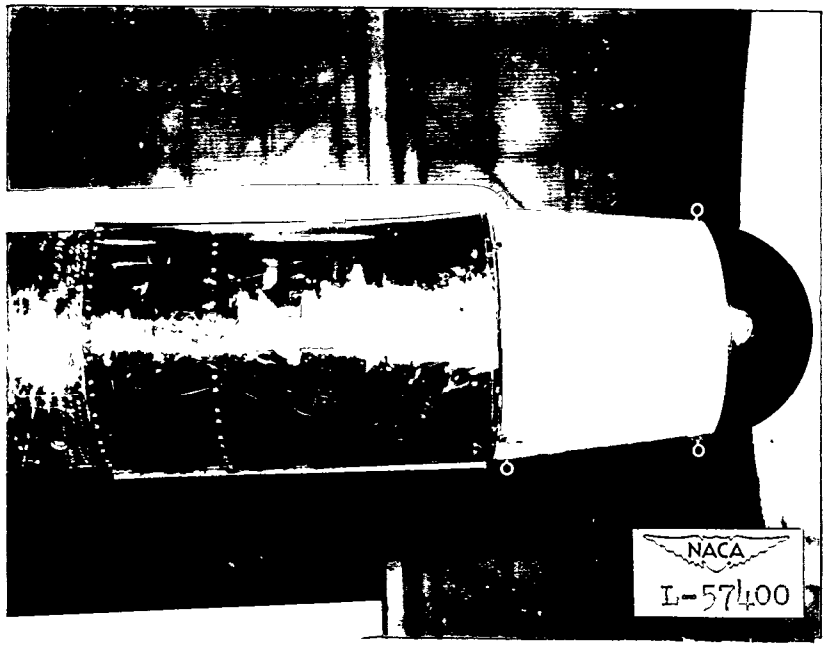

(a) Basic nose section.

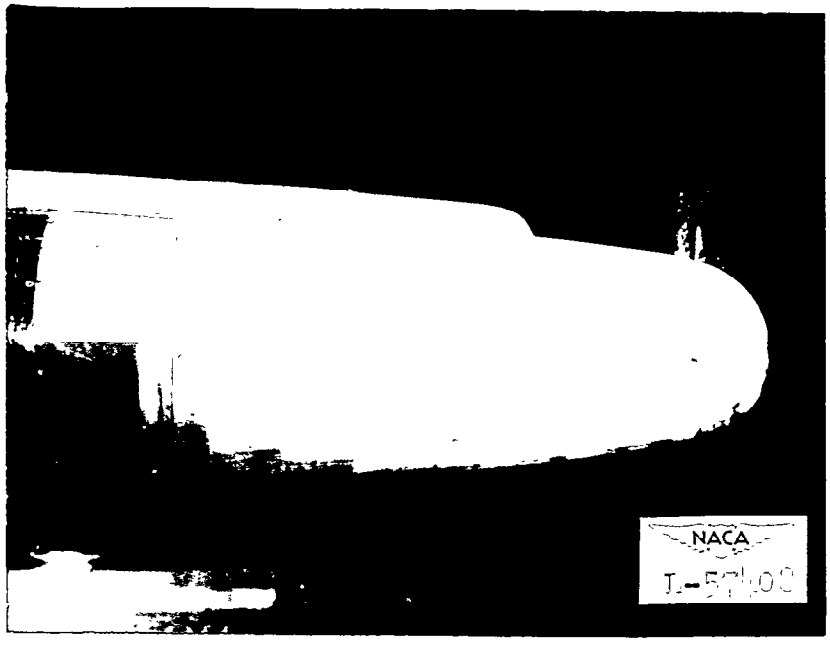

(b) Modified nose section.

Figure 6.– Basic and modified nose sections.

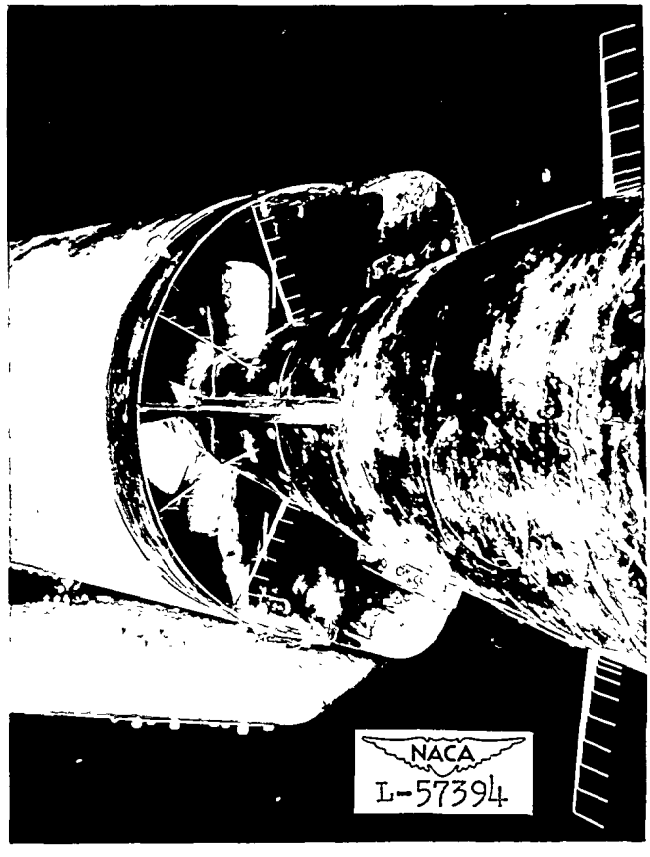

(a) Basic condition.

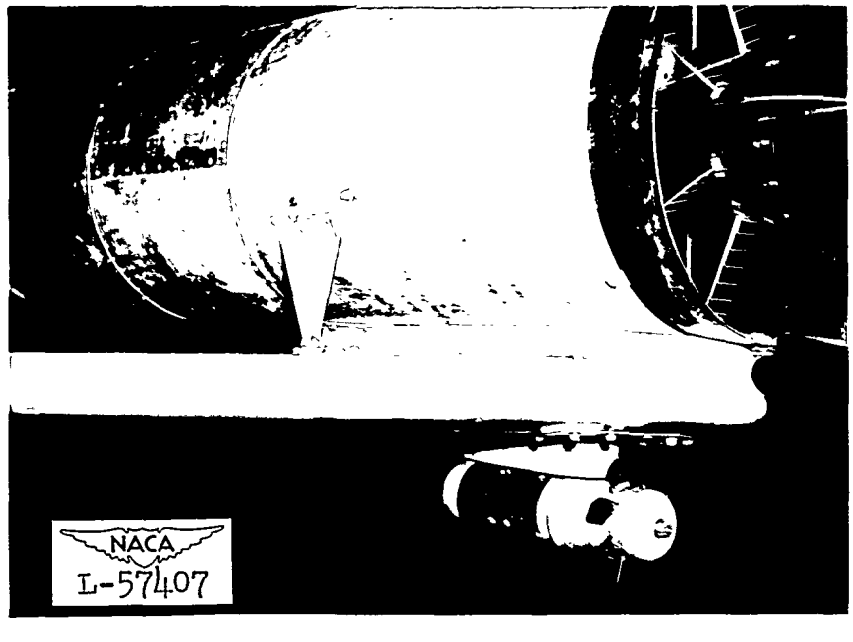

(b) Fillet installed.

Figure 7.- MK-13 horizontal-tail installation.

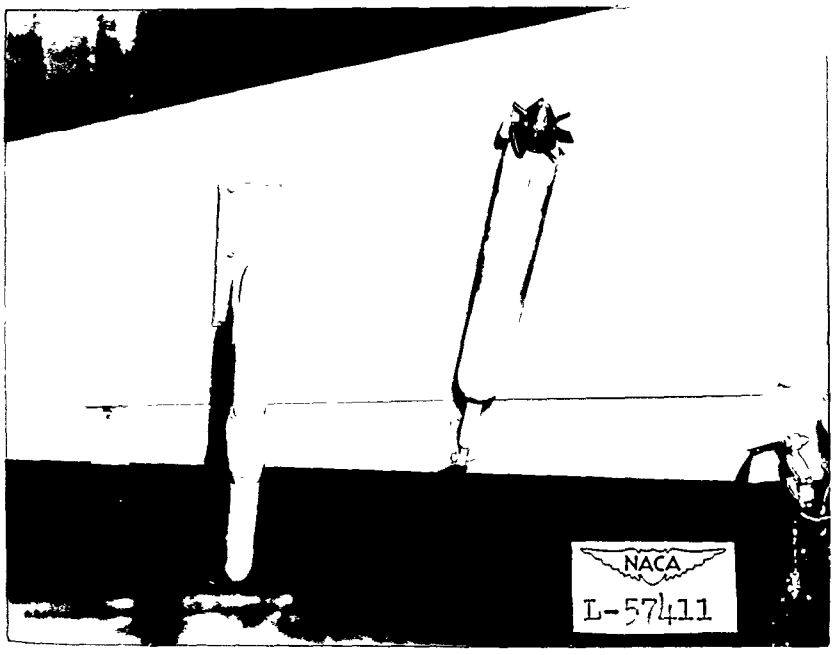

(a) Bottom view.

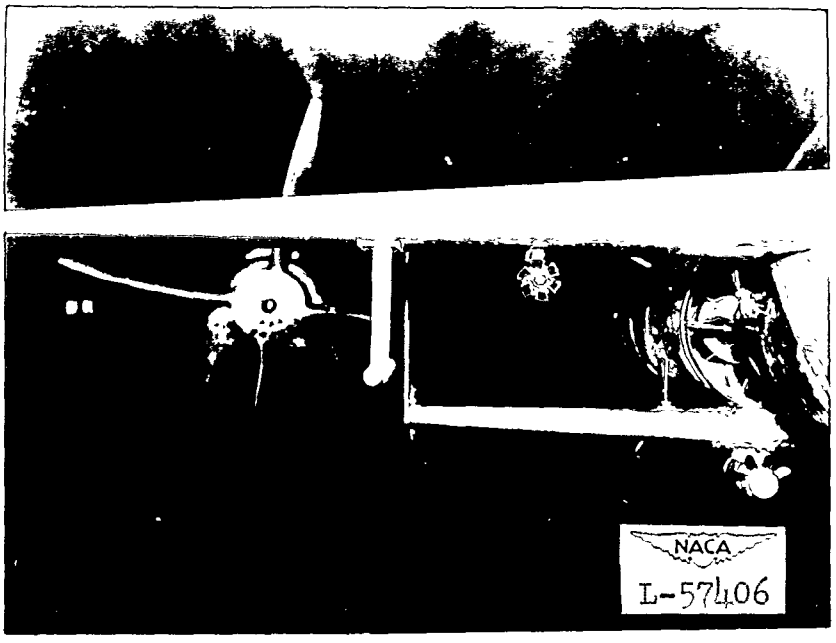

(b) Front view.

Figure 8.– Underwing actuator and altimeter antenna installation.

(a) MK-13 configuration.

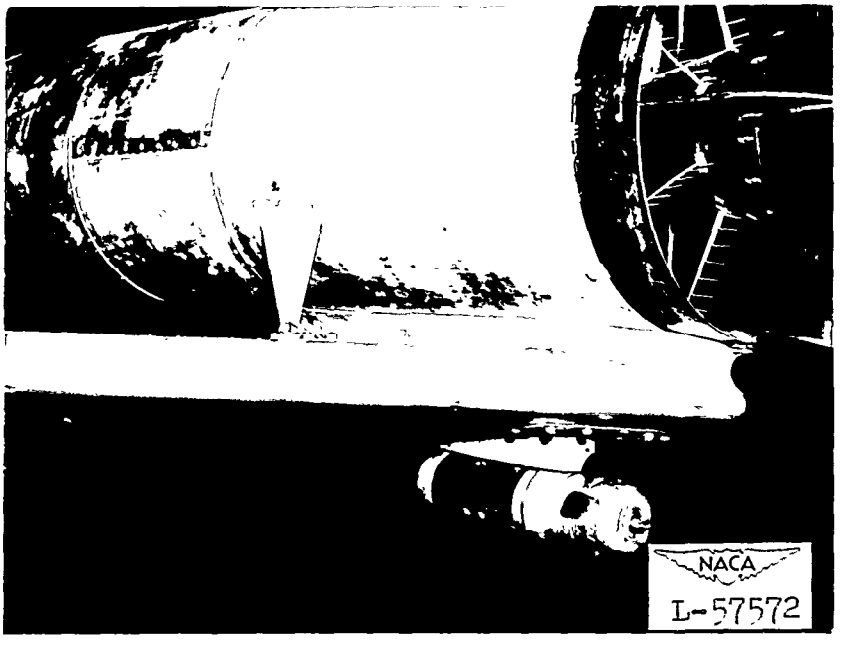

(b) MK-21 configuration.

Figure 9.- MK-13 and MK-21 tail configurations with fillets and auxiliary generator installed.

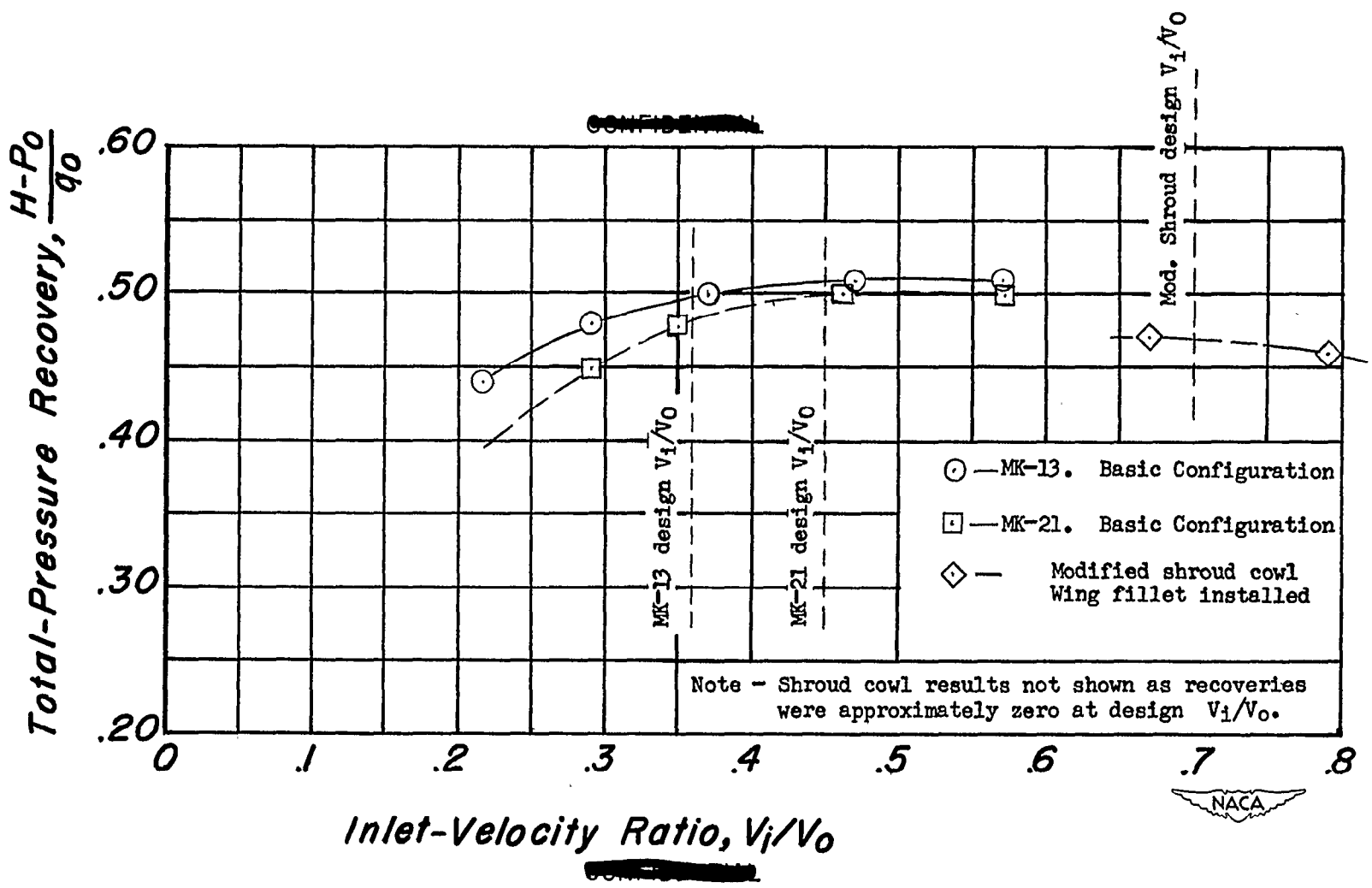

Figure 10.- Variation of total-pressure recovery with inlet-velocity ratio. α, -0.6°; R, 1.4×10^6.

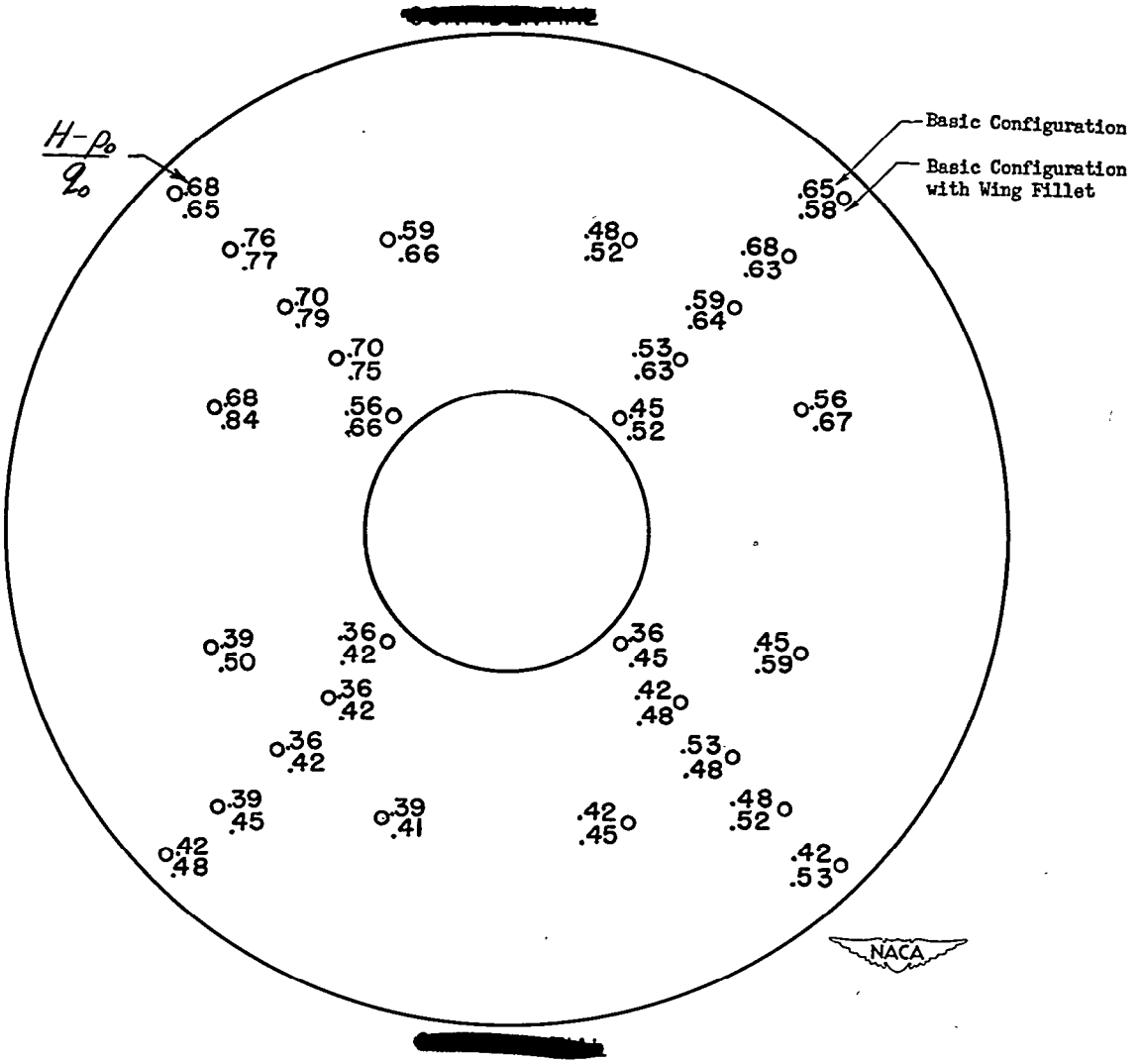

Figure 11.- Total-pressure distribution at the compressor inlet. MK-13 torpedo configuration; V_1/V_0, 0.36; α, -0.6°; R, 1.4×10^6.

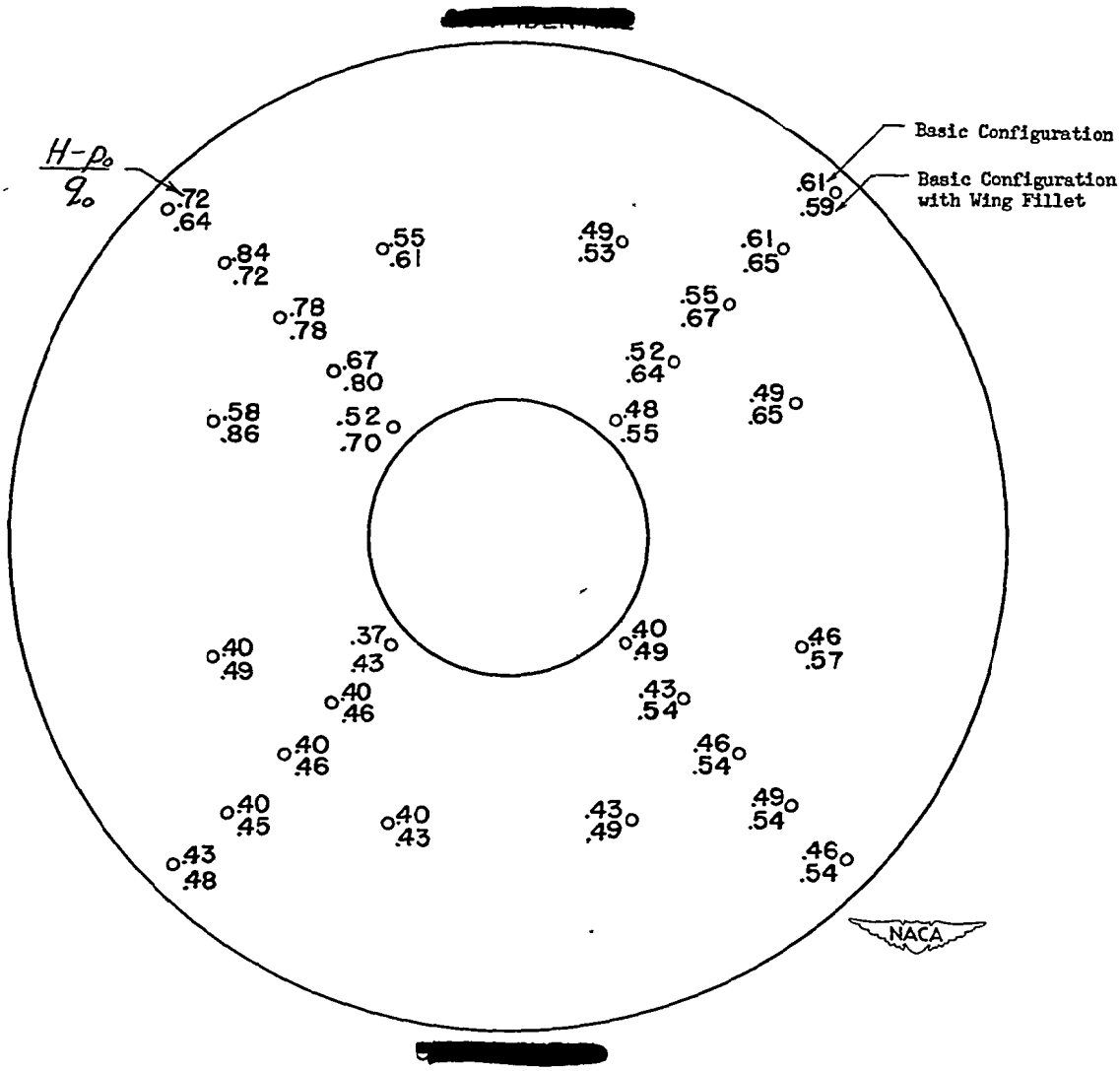

Figure 12.- Total-pressure distribution at the compressor inlet. MK-21 torpedo configuration; V_1/V_0, 0.45; α, -0.6°; R, 1.4×10^6.

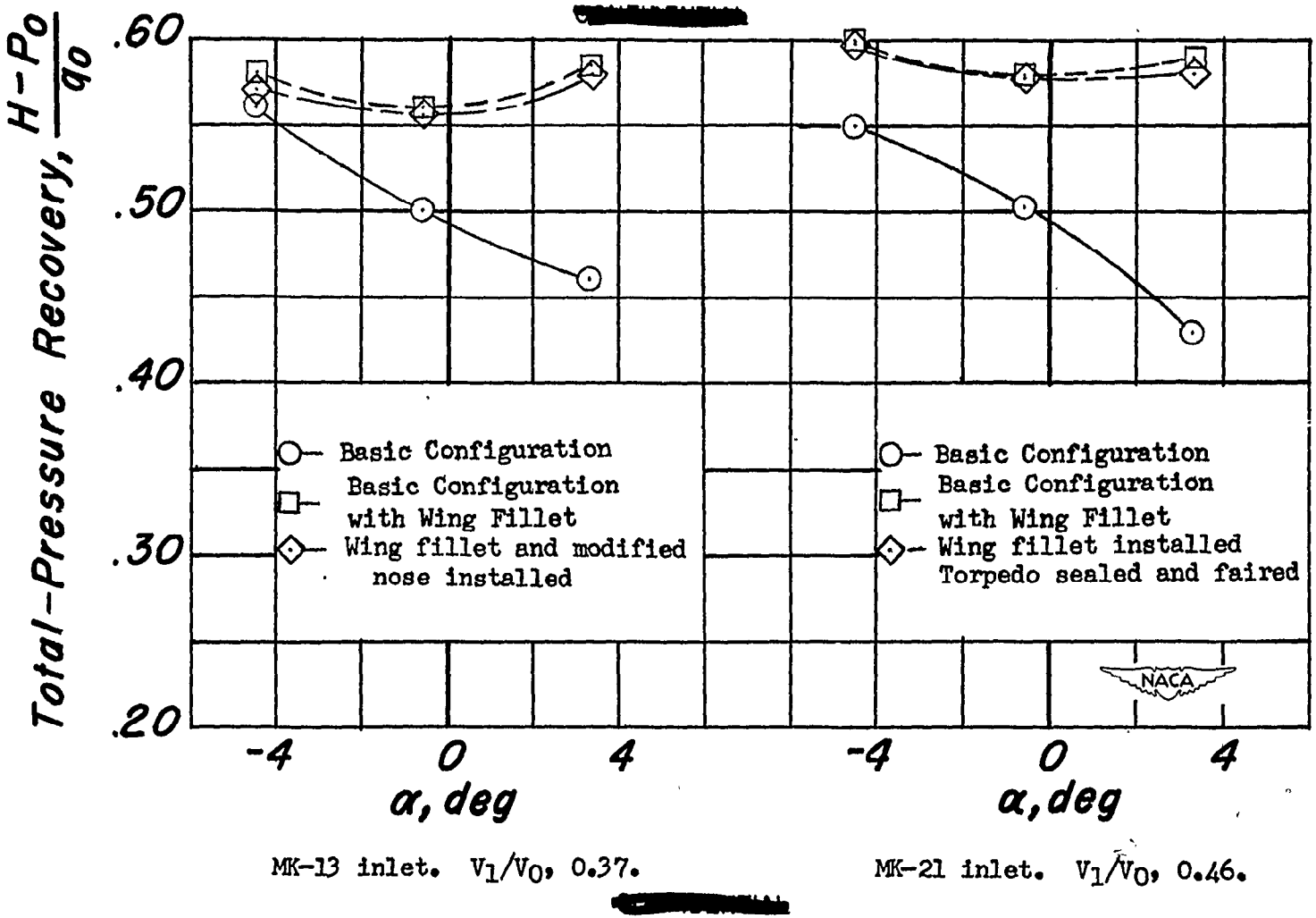

Figure 13.- Variation of total-pressure recovery with angle of attack. R, 1.4×10^6.

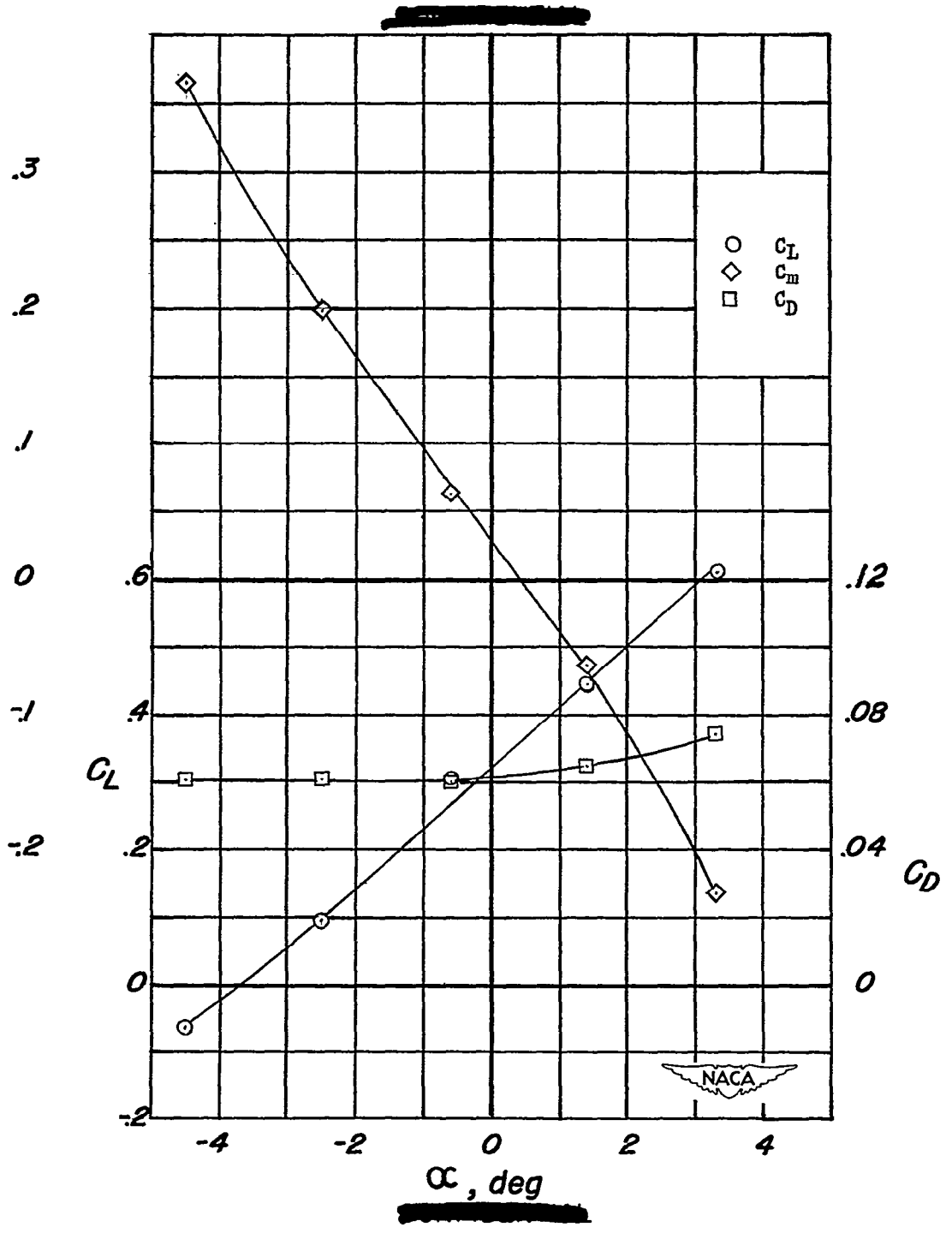

Figure 14.– Aerodynamic characteristics of basic model. δ_e, 0; δ_t, 0; i_t, 0.

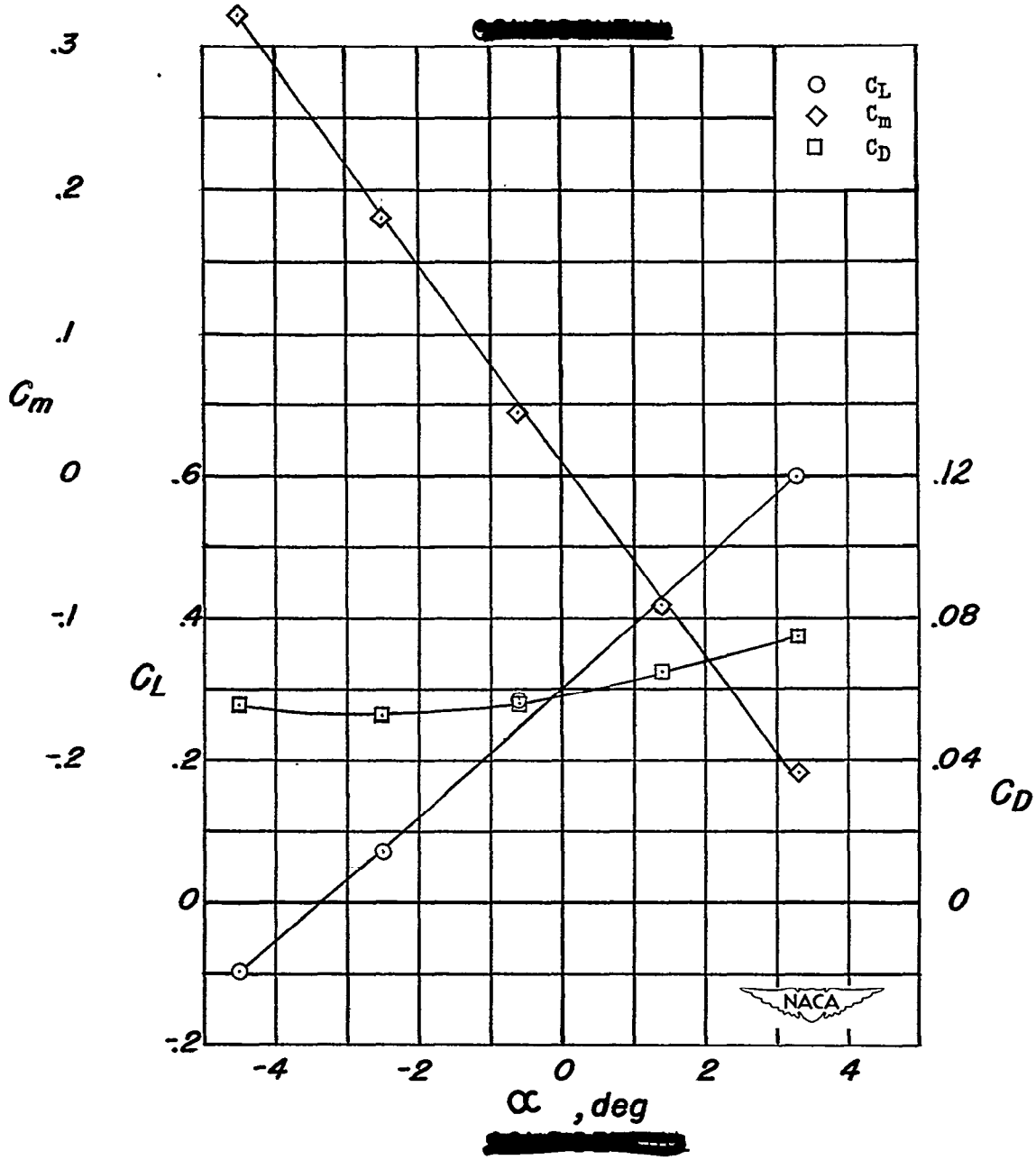

Figure 15.– Aerodynamic characteristics of model with wing fillet installed. δ_e, 0; δ_t, 0; i_t, 0.

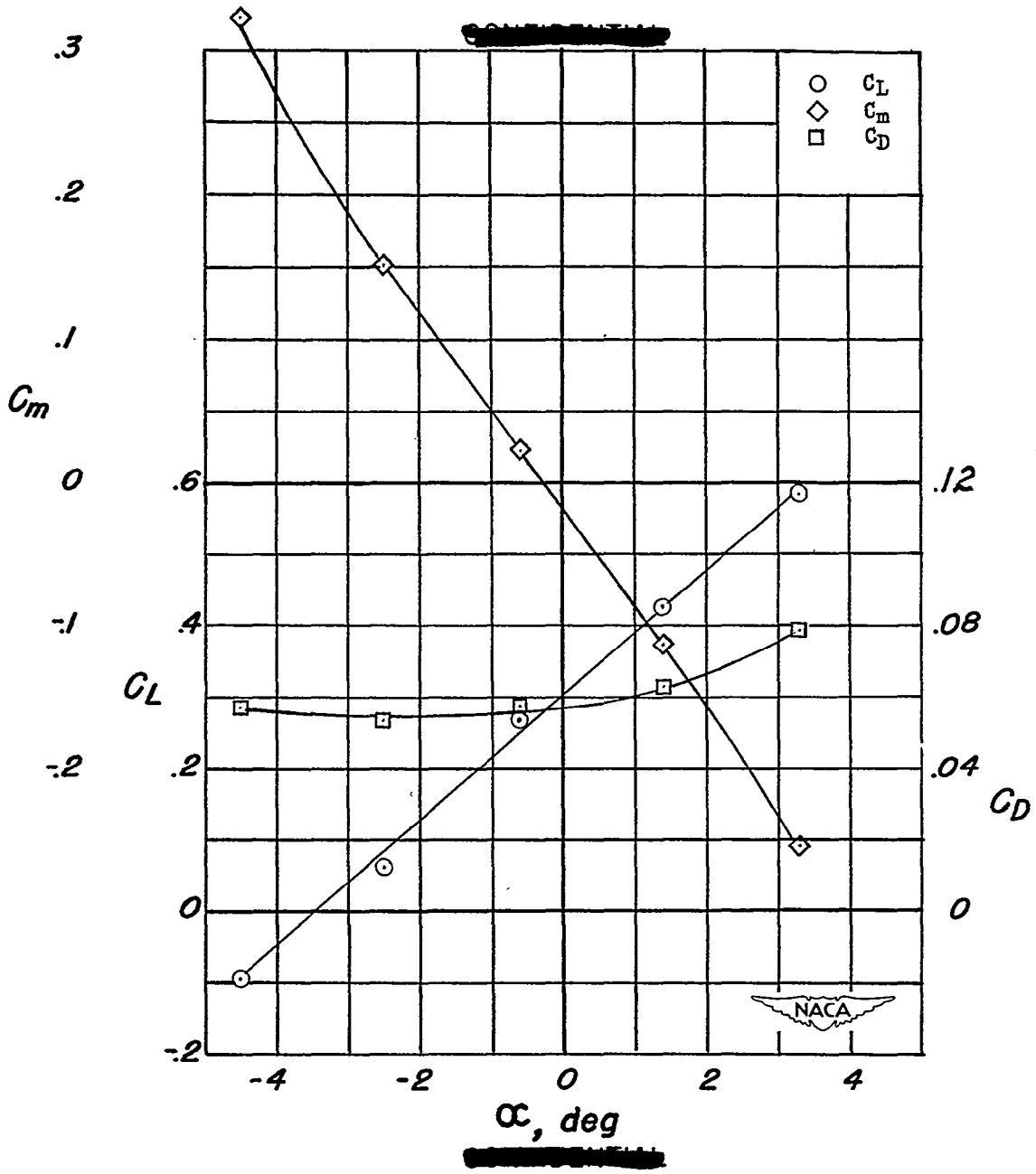

Figure 16.— Aerodynamic characteristics of model with wing fillet and tail fillet installed. δ_e, 0; δ_t, 0; i_t, 0.

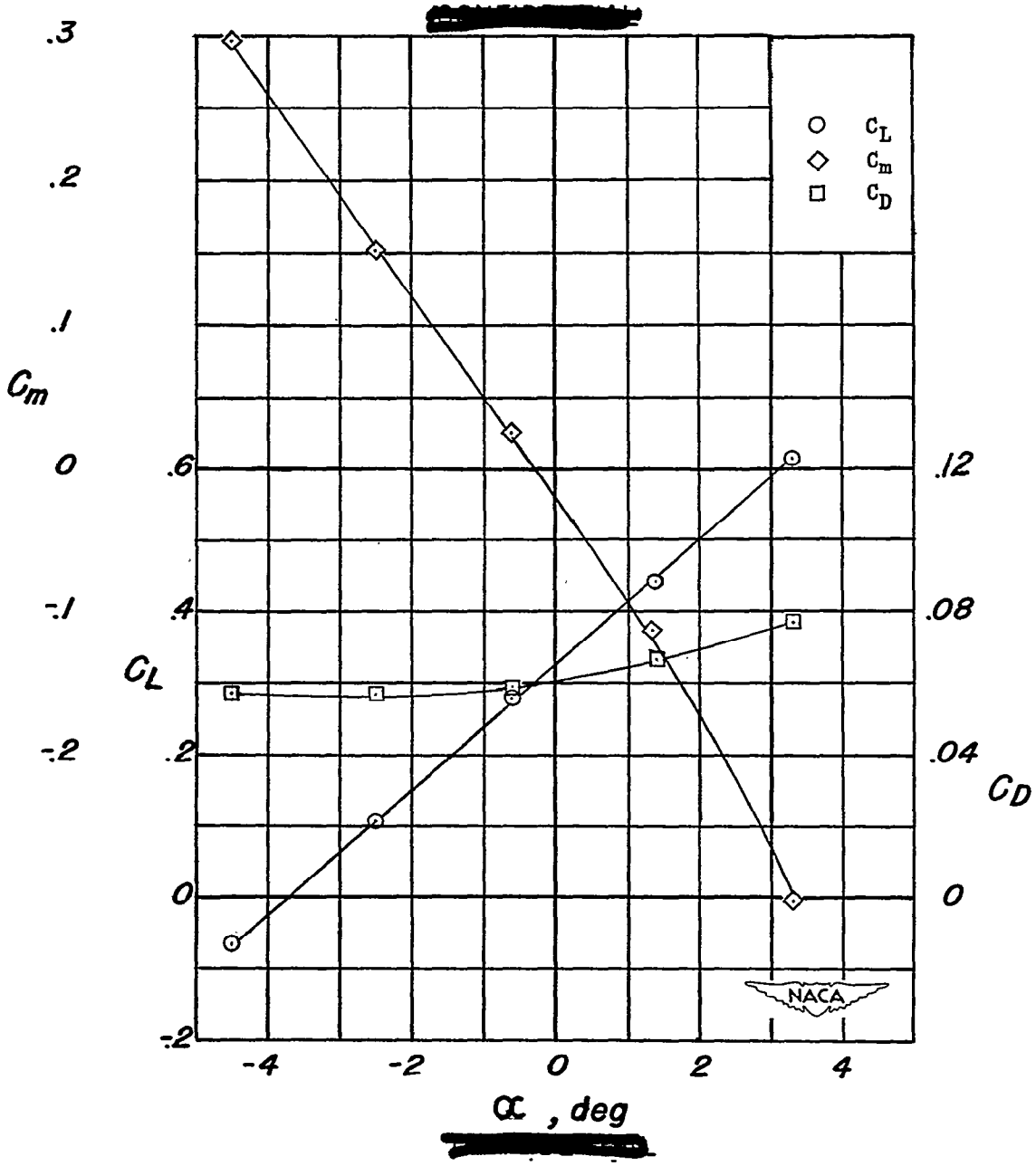

Figure 17.– Aerodynamic characteristics of model with wing fillet, tail fillet, and underwing actuator installed. δ_e, 0; δ_t, 0; i_t, 0.

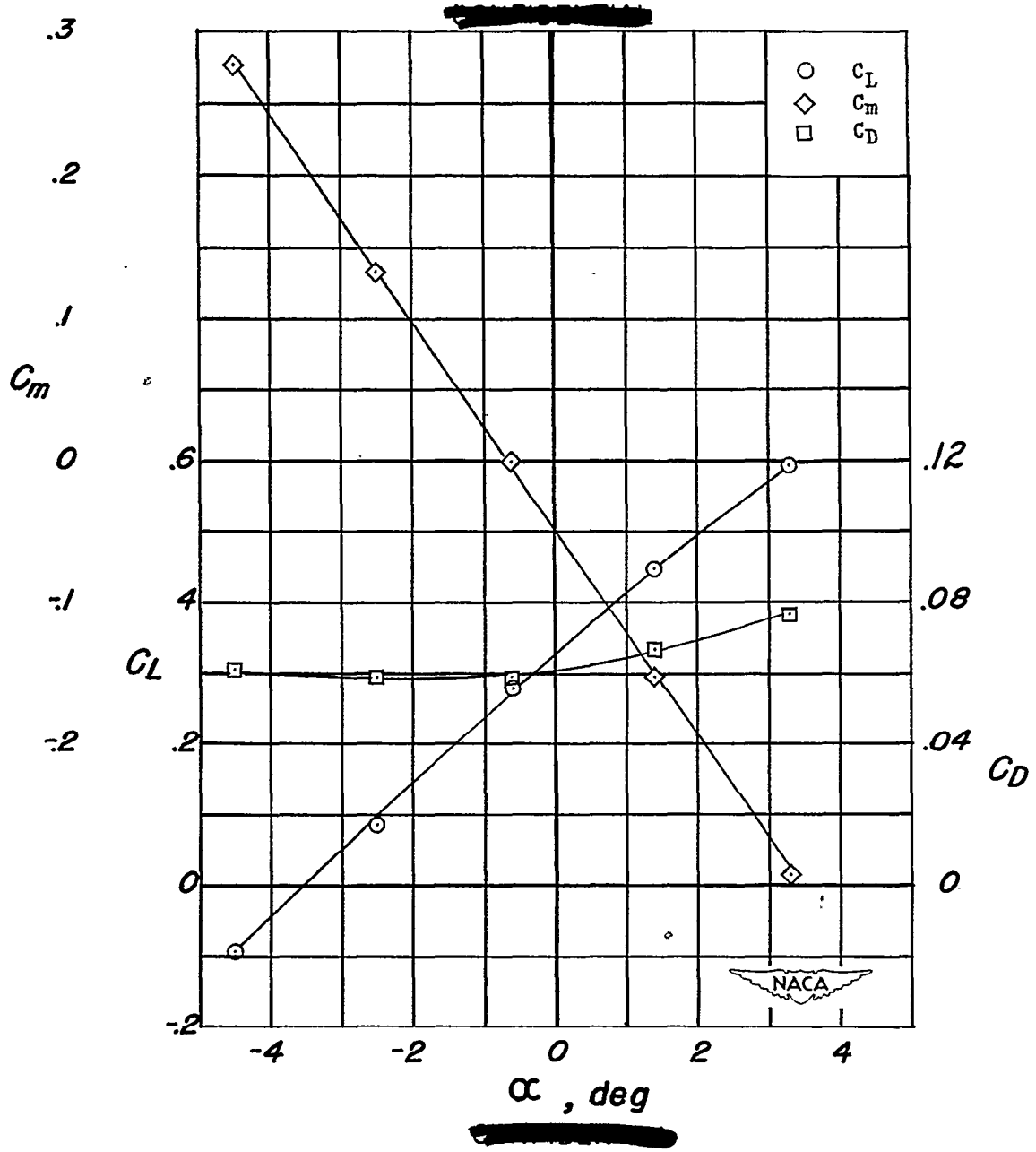

Figure 18.– Aerodynamic characteristics of model with wing fillet, tail fillet, underwing actuator, and altimeter antenna installed. δ_e, 0; δ_t, 0; i_t, 0.

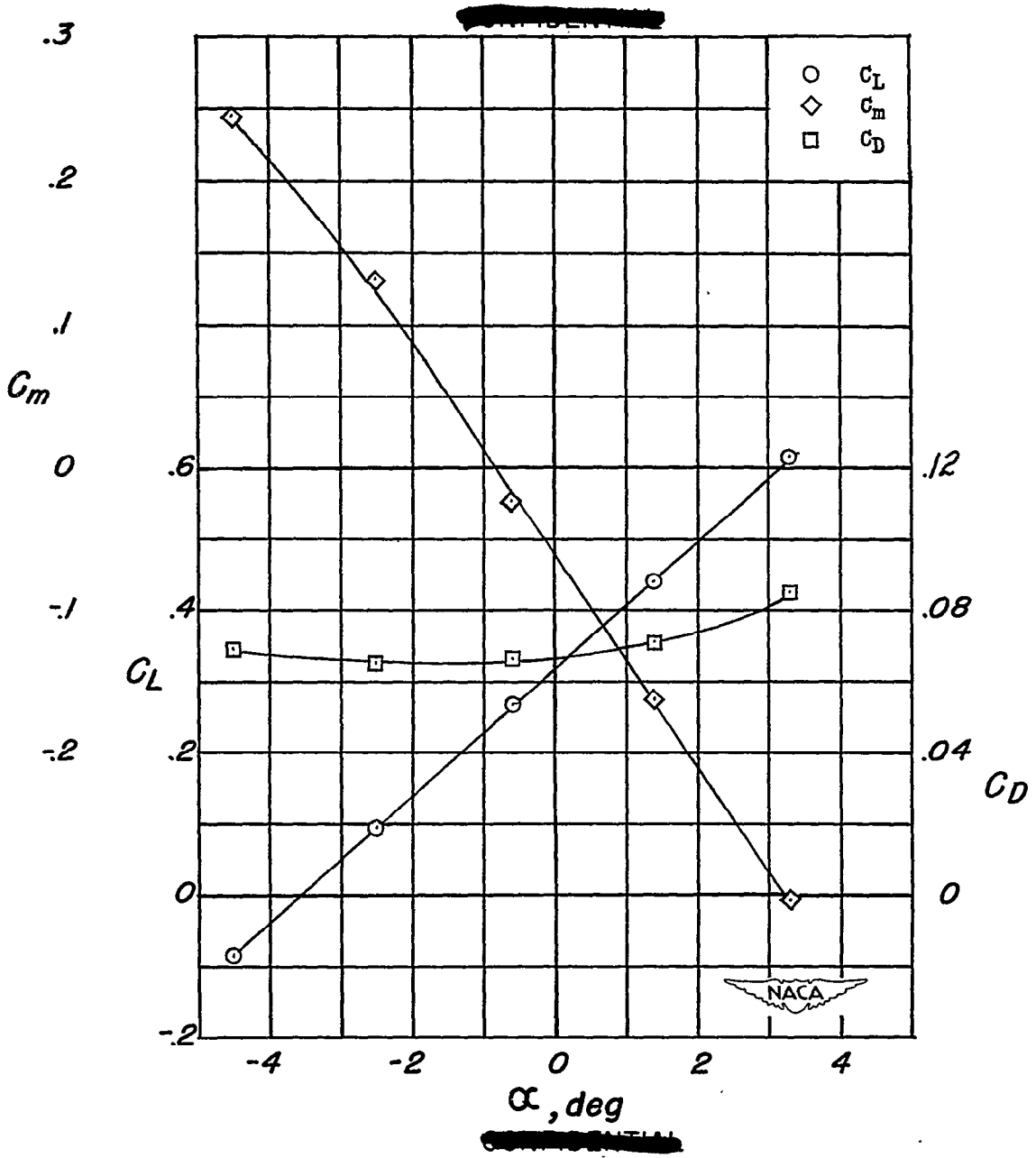

Figure 19.— Aerodynamic characteristics of model with wing fillet, tail fillet, underwing actuator, altimeter antenna, and wind generator installed. δ_e, 0; δ_t, 0; i_t, 0.

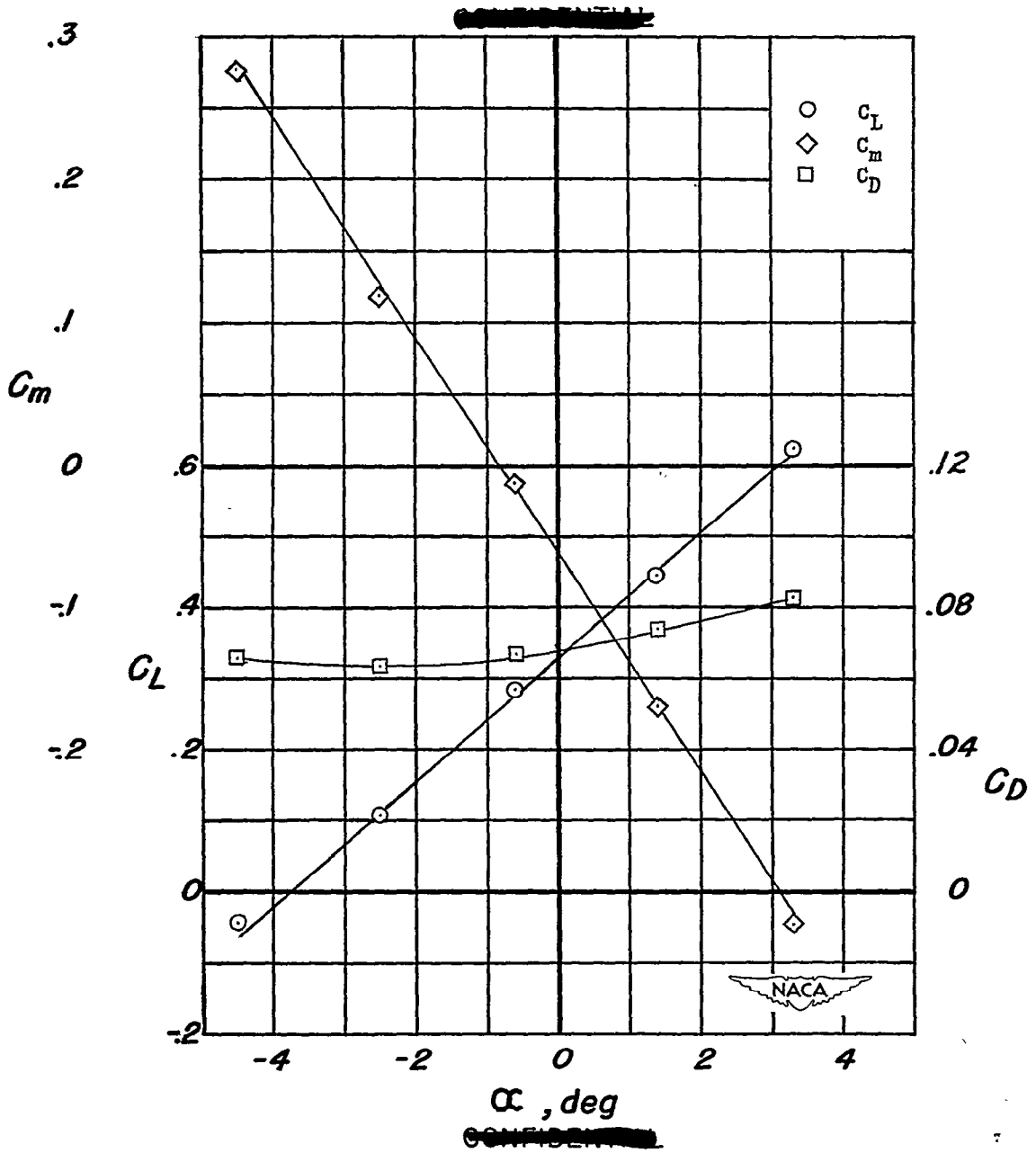

Figure 20.– Aerodynamic characteristics of model with wing fillet, tail fillet, underwing actuator, altimeter antenna, wind generator, and modified nose installed. δ_e, 0; δ_t, 0; i_t, 0.

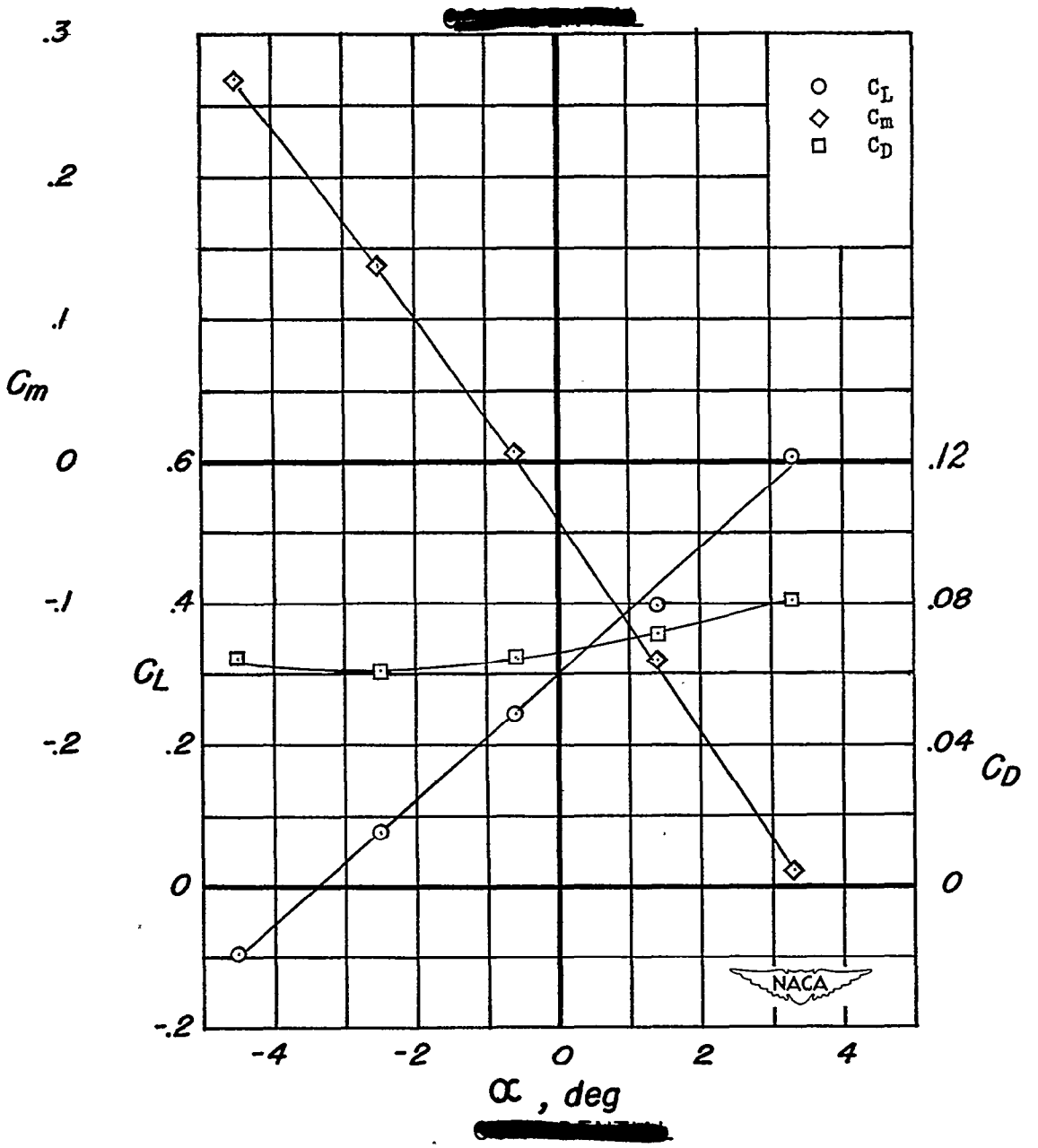

Figure 21.– Aerodynamic characteristics of model with wing fillet, tail fillet, underwing actuator, altimeter antenna, wind generator, modified nose, and MK-21 tail configuration installed. δ_e, 0; δ_t, 0; i_t, 0.

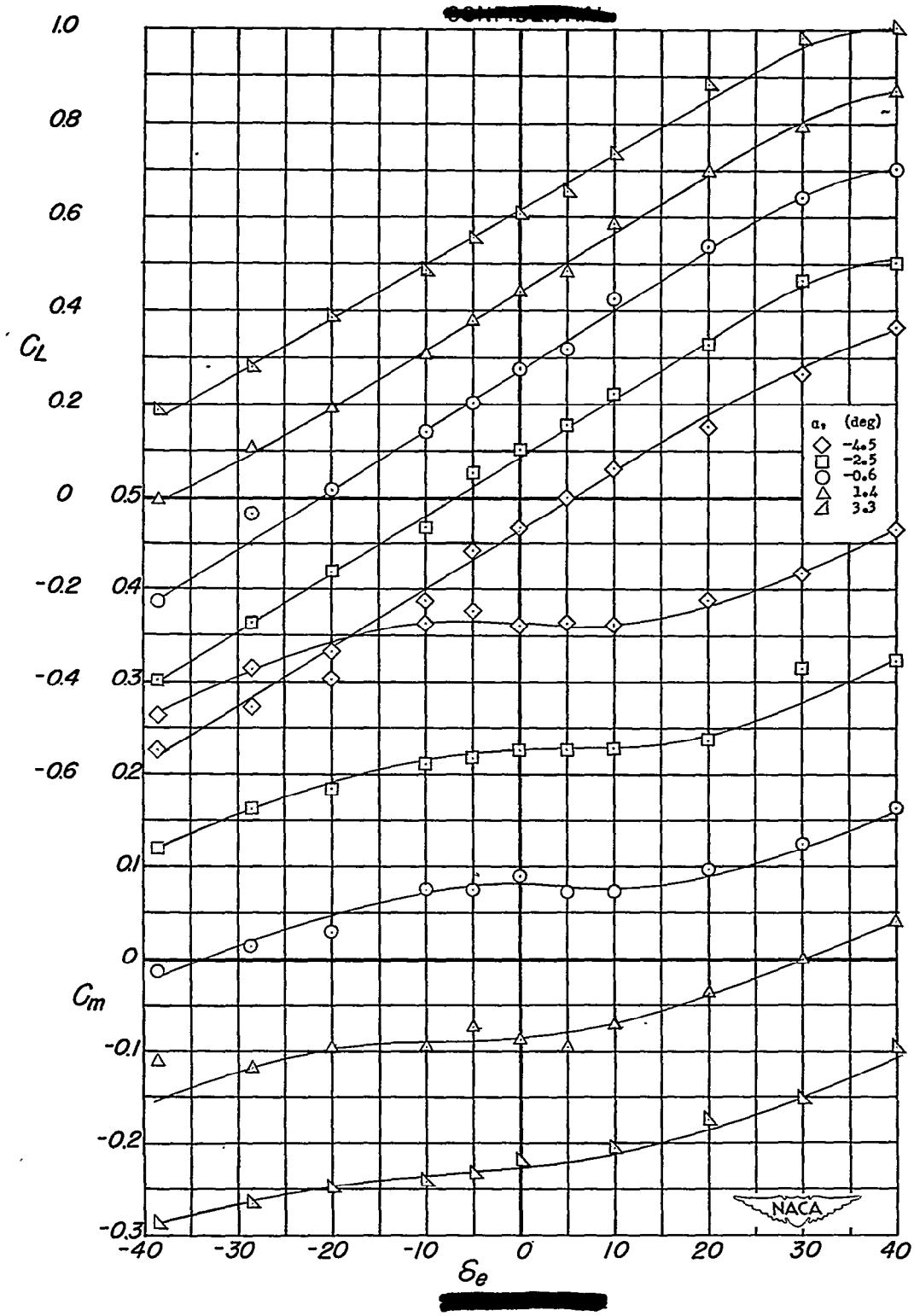

Figure 22.– Variation of lift, drag, and pitching-moment coefficients with elevon deflection. MK-13 basic configuration; δ_t, 0°; i_t, 0°.

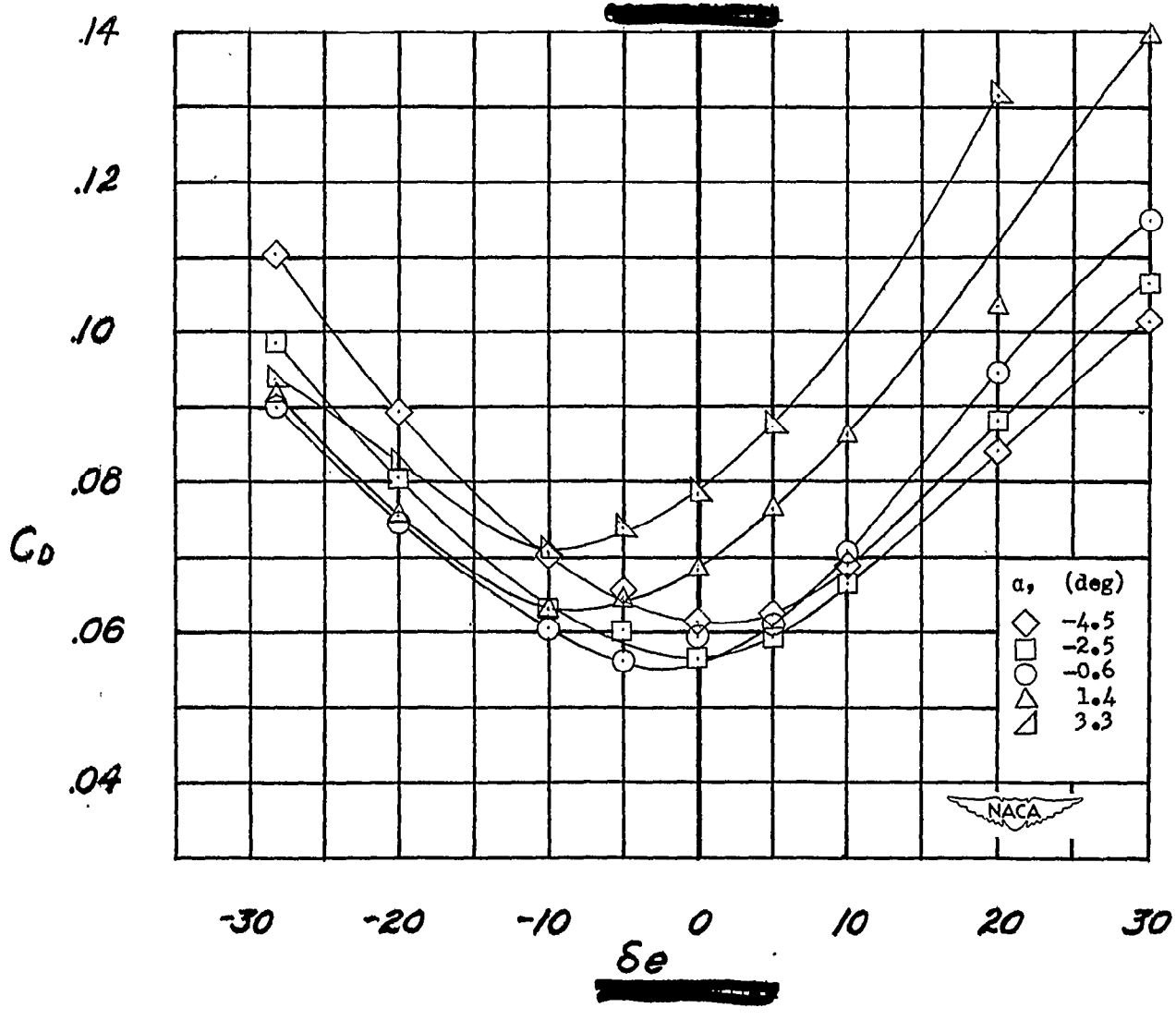

Figure 22.- Concluded.

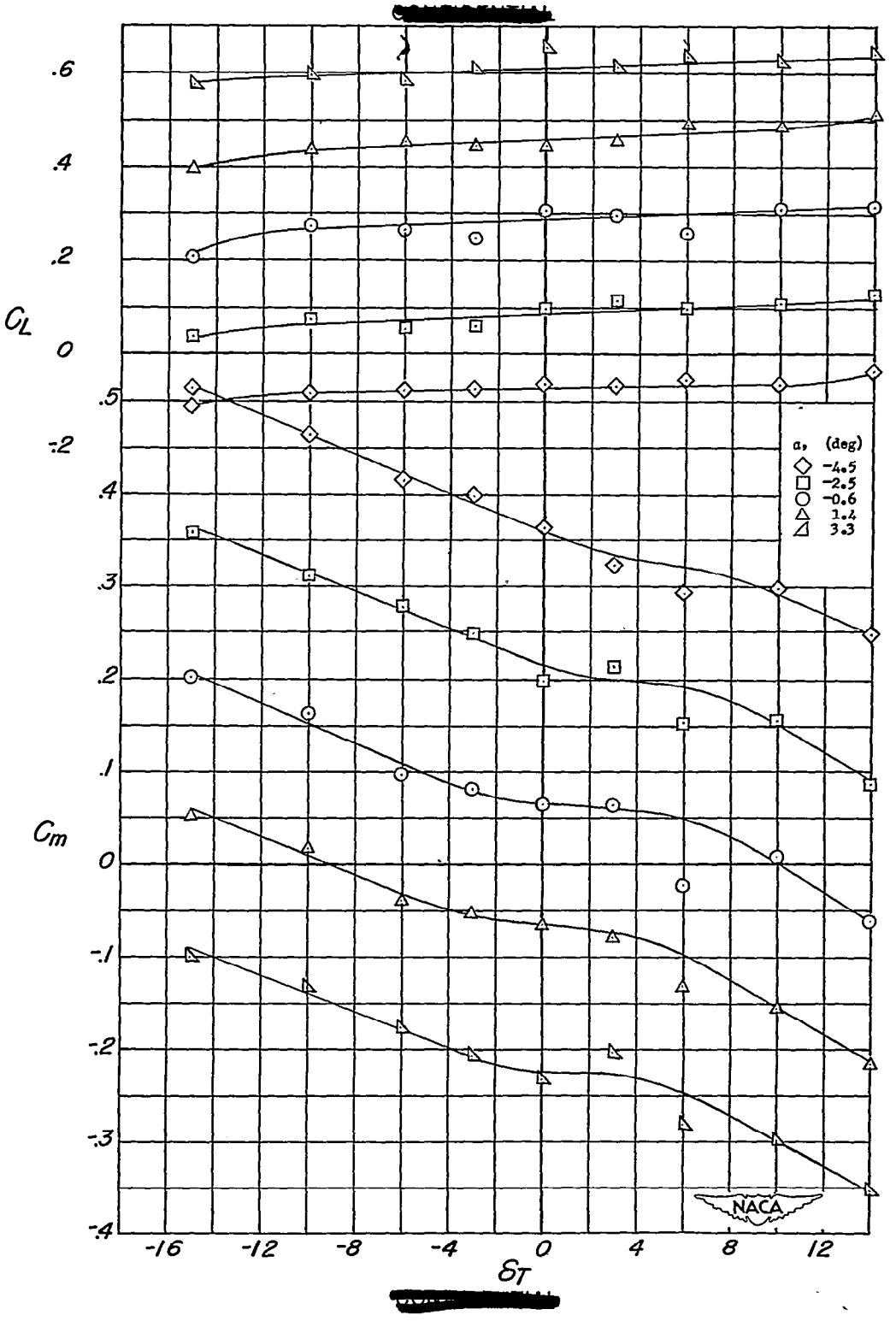

Figure 23.— Variation of lift, drag, and pitching-moment coefficients with tab deflection. MK-13 basic configuration; δ_e, 0°; i_t, 0°.

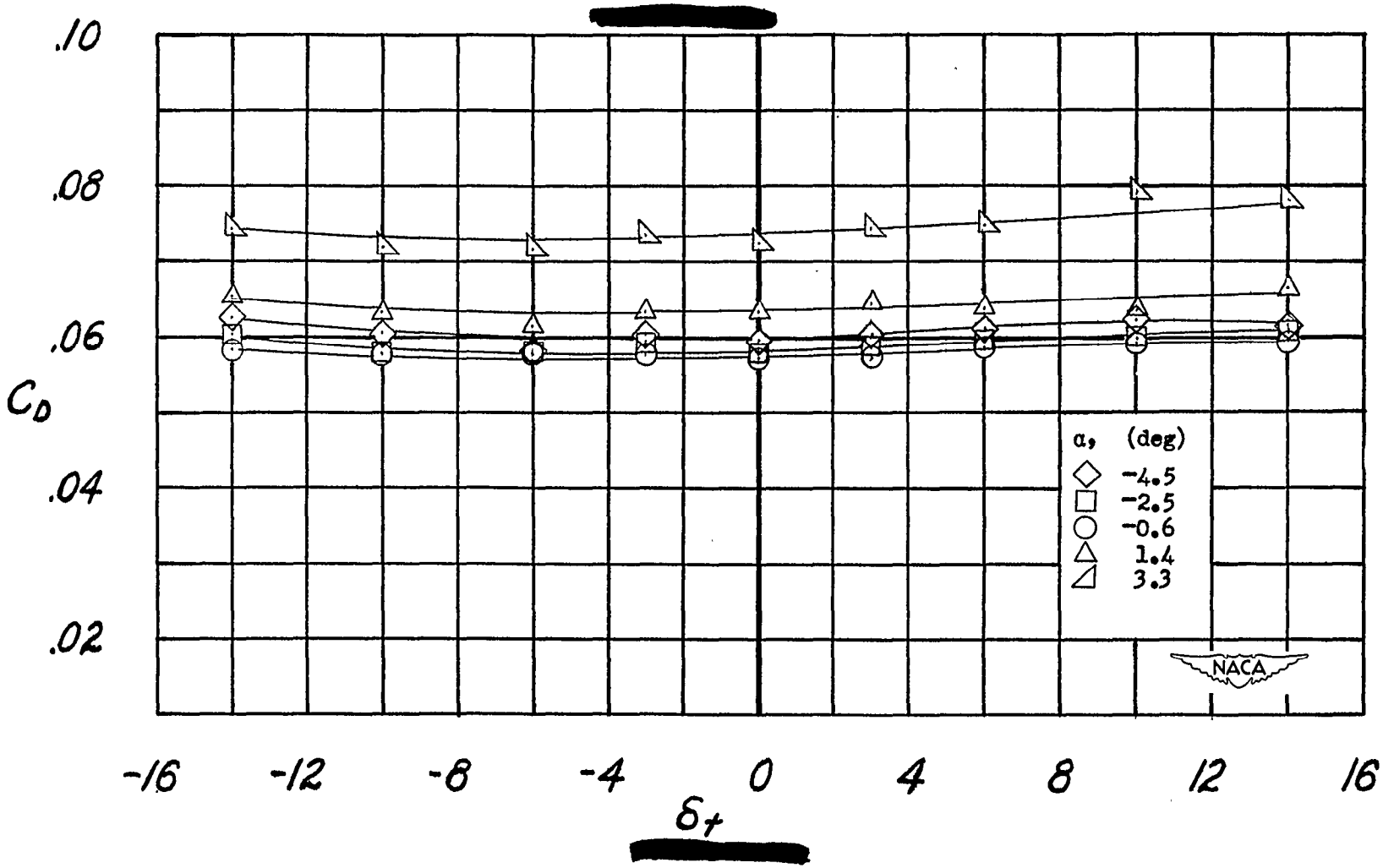

Figure 23.– Concluded.

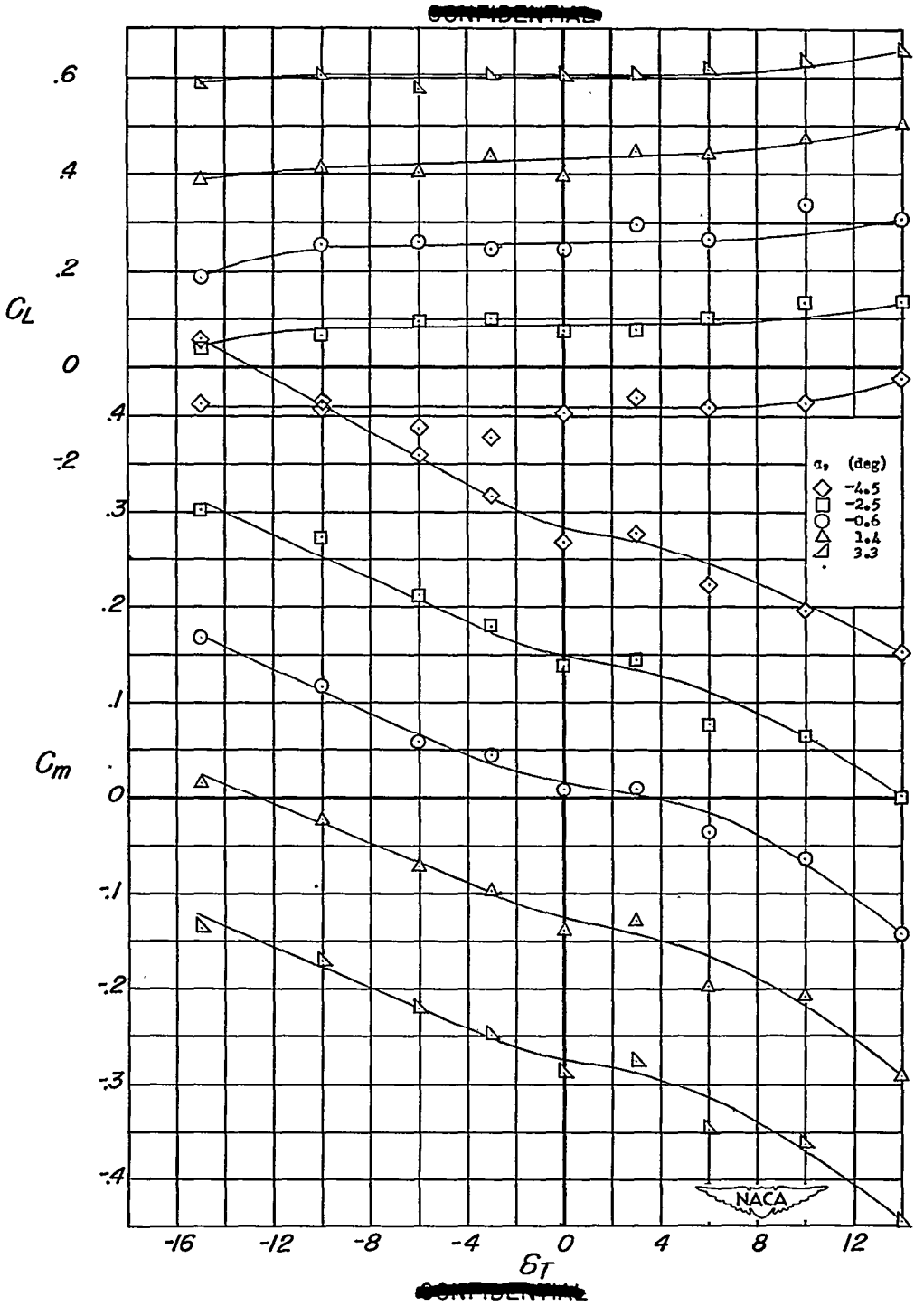

Figure 24.– Variation of lift, drag, and pitching-moment coefficients with tab deflection. MK-21 configuration with wing fillet, tail fillet, actuators, altimeter antennas, and wind generator installed; δ_e, 0°; i_t, 0°.

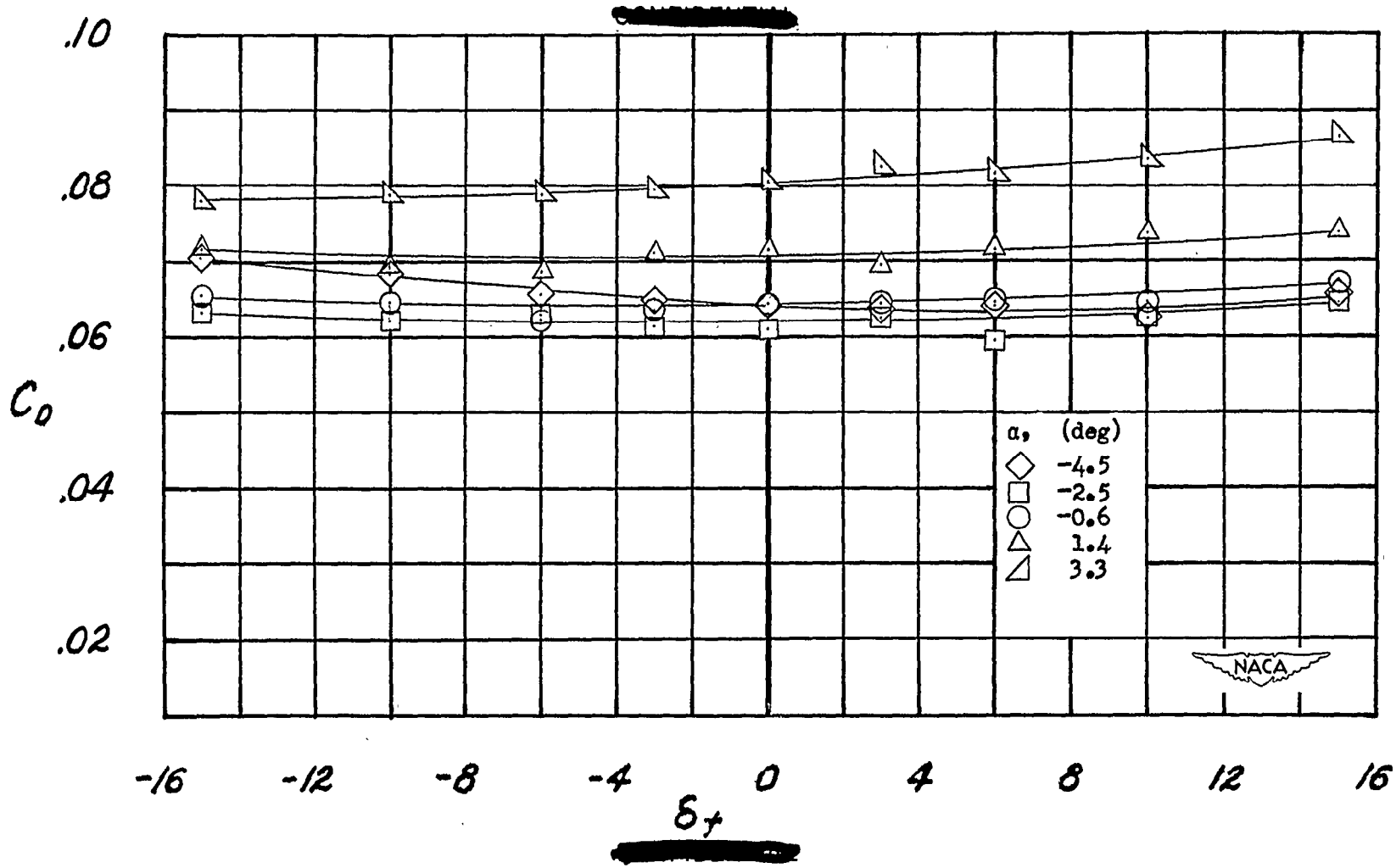

Figure 24.– Concluded.

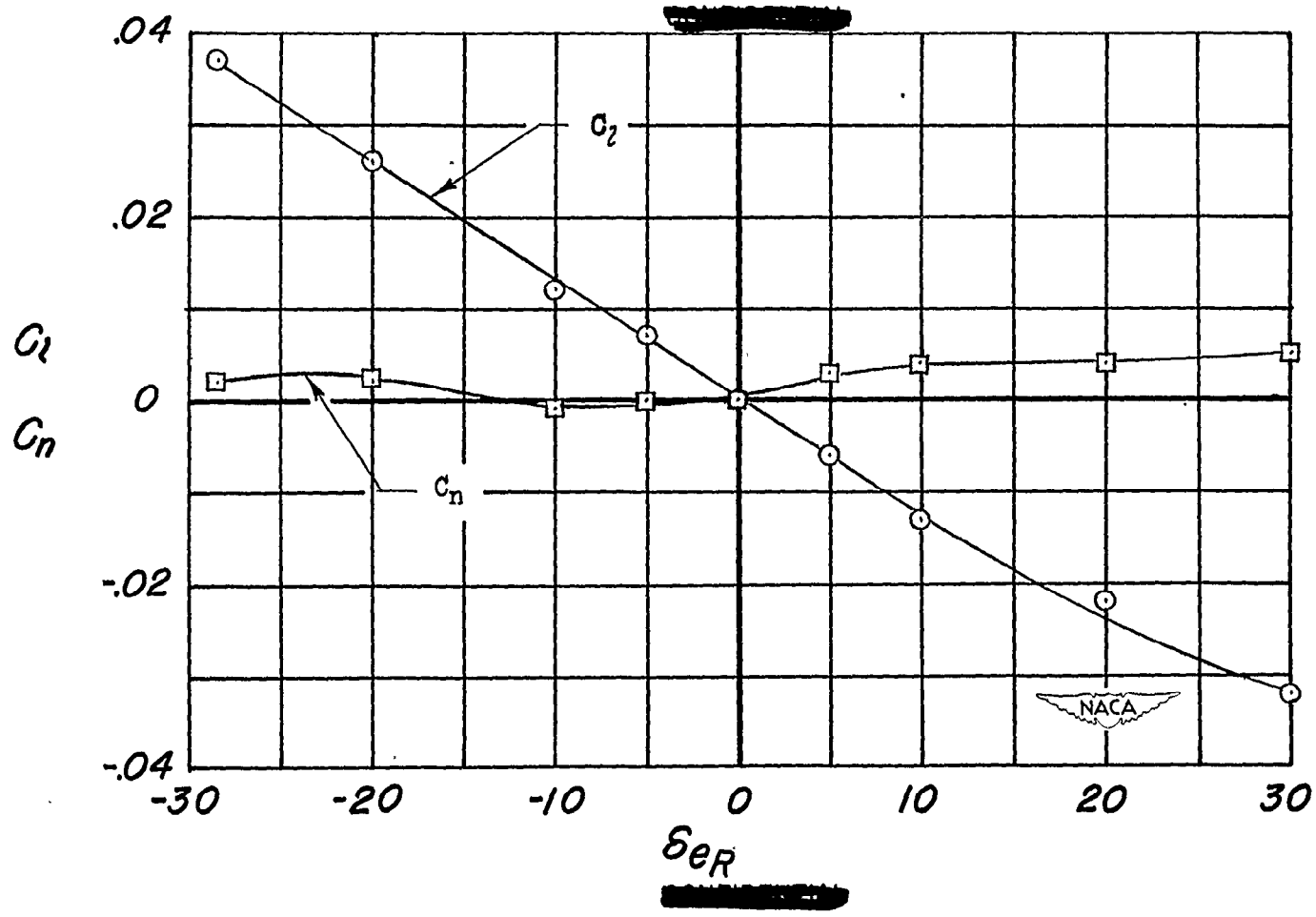

Figure 25.– Variation of rolling-and yawing-moment coefficients with aileron deflection. δ_t, 0°; i_t, 0°; α, –0.6°.

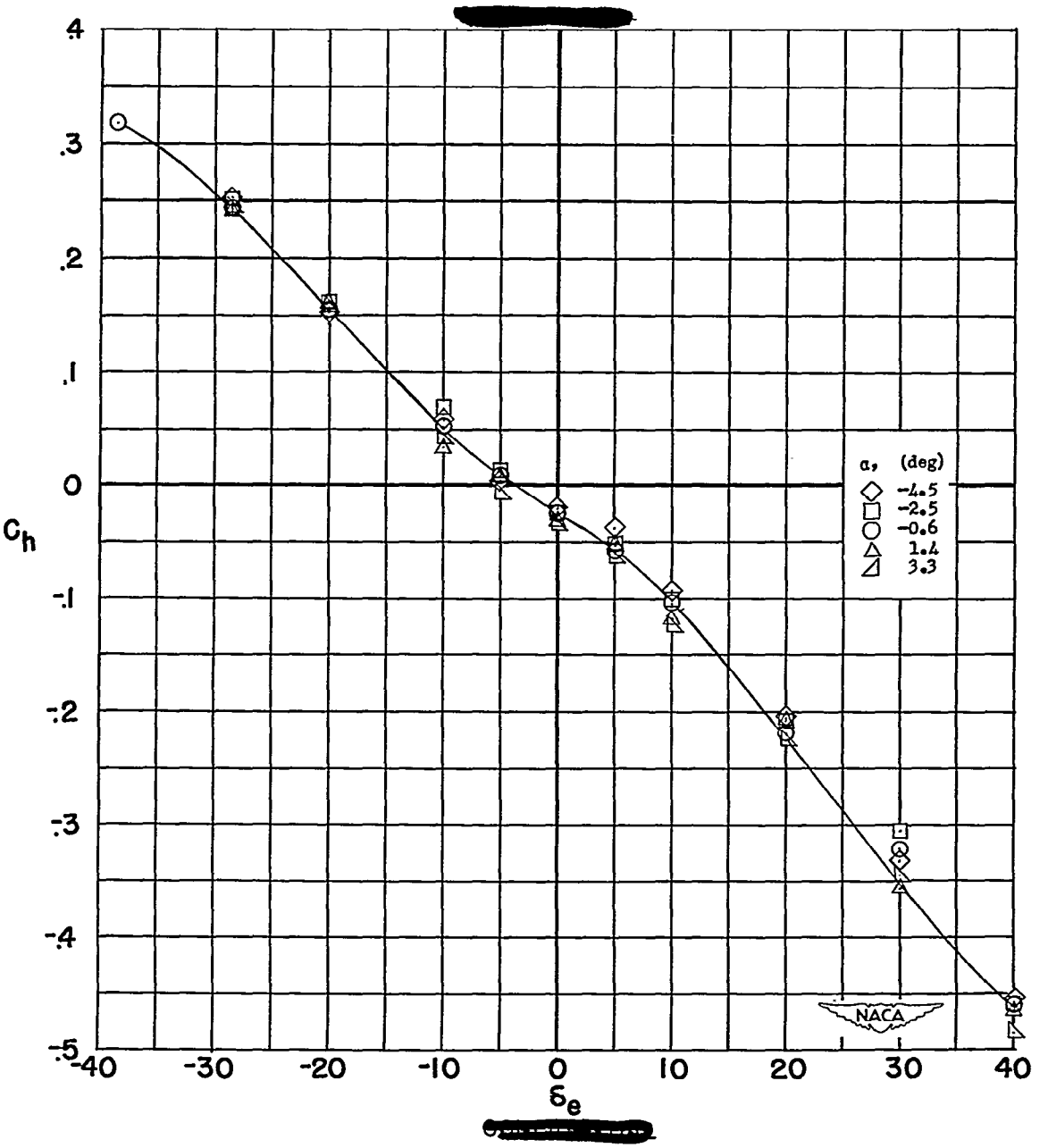

Figure 26.– Variation of elevon hinge moments with elevon deflection. δ_t, 0°; i_t, 0°.